© 2016. Published by The Company of Biologists Ltd | Journal of Cell Science (2016) 129, 621-636 doi:10.1242/jcs.179713

RESEARCH ARTICLE

WDR8 is a centriolar satellite and centriole-associated protein that promotes ciliary vesicle docking during ciliogenesis

Bahtiyar Kurtulmus[1,2,‡], Wenbo Wang[2,3,‡], Thomas Ruppert[3], Annett Neuner[3], Berati Cerikan[3], Linda Viol[1,2], Rafael Dueñas-Sánchez[2], Oliver J. Gruss[3,*,§] and Gislene Pereira[1,2,§]

ABSTRACT

Ciliogenesis initiates at the mother centriole through a series of events that include membrane docking, displacement of cilia-inhibitory proteins and axoneme elongation. Centriolar proteins, in particular at distal and subdistal appendages, carry out these functions. Recently, cytoplasmic complexes named centriolar satellites have also been shown to promote ciliogenesis. Little is known about the functional and molecular relationship between appendage proteins, satellites and cilia biogenesis. Here, we identified the WD-repeat protein 8 (WDR8, also known as WRAP73) as a satellite and centriolar component. We show that WDR8 interacts with the satellite proteins SSX2IP and PCM1 as well as the centriolar proximal end component Cep135. Cep135 is required for the recruitment of WDR8 to centrioles. Depletion experiments revealed that WDR8 and Cep135 have strongly overlapping functions in ciliogenesis. Both are indispensable for ciliary vesicle docking to the mother centriole and for unlocking the distal end of the mother centriole from the ciliary inhibitory complex CP110–Cep97. Our data thus point to an important function of centriolar proximal end proteins in ciliary membrane biogenesis, and establish WDR8 and Cep135 as two factors that are essential for the initial steps of ciliation.

KEY WORDS: Cilia, Satellites, Centrosomes, Basal body, SSX2IP, WDR8, WRAP73, Cep135

INTRODUCTION

The centrosome is the main microtubule-organising centre (MTOC) of most animal cells. Centrosomes generally consist of two orthogonally arranged centrioles surrounded by layers of pericentriolar material (PCM). Centrioles bear a defined structure of nine triplet microtubules of defined length. In addition, one of the two centrioles of the pair acquires appendage proteins that assemble at the subdistal and distal ends of the centriole. The centriole associated with appendage proteins is called the mother centriole. The daughter centriole lacks appendage proteins. When cells exit mitosis and withdraw from the cell cycle, for example, upon differentiation, the mother centriole turns into the basal body that functions as a platform for the formation of a single non-motile cilium (primary cilium). Primary cilia serve as mechano- and chemo-sensing organelles. They consist of a bundle of axonemal microtubules surrounded by the ciliary membrane. The latter accumulates a number of membrane receptors, which detect environmental cues with high sensitivity (Singla and Reiter, 2006; Ishikawa and Marshall, 2011; Kim and Dynlacht, 2013). A rising number of mutations in genes coding for ciliary proteins cause a variety of genetic disorders that collectively are called 'ciliopathies'. Ciliopathies are often a consequence of impaired signalling functions of primary cilia. Hence, understanding the molecular basis of primary cilia formation is of the highest medical relevance (Badano et al., 2006; Fliegauf et al., 2007; Baker and Beales, 2009).

Assembly of the primary cilium starts at the mother centriole with the docking of ciliary vesicles, most likely derived from the Golgi (Das and Guo, 2011; Qin, 2012). Distal appendage proteins, including Cep164 and Cep123 (also known as Cep89), have been reported to be indispensable for this initial step of ciliary membrane biogenesis (Schmidt et al., 2012; Tanos et al., 2013; Joo et al., 2013; Sillibourne et al., 2013; Burke et al., 2014; Ye et al., 2014). Moreover, a cascade of small GTPases regulates vesicle docking and fusion at the mother centriole. The GTPase Rab11 targets Rabin8 (also known as RAB3IP), a guanine nucleotide exchange factor (GEF) for the GTPase Rab8, to centrioles. Rabin8 activates Rab8 at the distal end of centrioles leading to vesicle extension (Knodler et al., 2010; Westlake et al., 2011). Recently, the membrane-shaping proteins EHD1 and EHD3, together with the SNARE SNAP29, have been shown to drive vesicle fusion and tubulation of ciliary vesicles (Lu et al., 2015). Following the assembly of the ciliary membrane, the CP110–Cep97 complex (which inhibits axonemal extension) is removed from the distal end of the centrioles (Spektor et al., 2007; Tsang et al., 2008). The microtubule triplets of the basal body then serve as seeds for the elongation of the axonemal microtubules.

Assembly of primary cilia, as well as their maintenance, requires constant exchange between cytoplasmic and centriolar components. Accumulating evidence indicates that macromolecular assemblies of centriolar proteins (known as centriolar satellites) actively support the communication of centrioles with the cytoplasm. Satellites assist centrosome rearrangements and diverse centriolar functions throughout the cell cycle and are involved in centriole duplication, mitotic spindle and primary cilia formation (Bärenz et al., 2011; Tollenaere et al., 2015). A number of proteins with known functions in ciliogenesis localise, at least in part, to centriolar satellites (Tollenaere et al., 2015). SSX2IP, PCM1 and Cep290 are satellite proteins that function in ciliogenesis (Jin et al., 2010; Klinger et al., 2014; Craige et al., 2010; Garcia-Gonzalo et al., 2011; Hori et al., 2014). How satellites are assembled and how they contribute to ciliogenesis is only rudimentarily understood.

Here, we have identified human WDR8 (also known as WRAP73) as an interacting partner of the satellite components

[1]Centre for Organismal Studies (COS), Im Neuenheimer Feld 230, Heidelberg 69120, Germany. [2]Division of Centrosomes and Cilia, German Cancer Research Centre (DKFZ), DKFZ-ZMBH Alliance, Im Neuenheimer Feld 581, Heidelberg 69120, Germany. [3]Zentrum für Molekulare Biologie der Universität Heidelberg (ZMBH), DKFZ-ZMBH Alliance, Im Neuenheimer Feld 282, Heidelberg 69120, Germany.
*Present address: Bonn University, Institute of Genetics, Karlrobert-Kreiten-Strasse 13, Bonn 53115, Germany.
‡These authors contributed equally to this work

§Authors for correspondence (gislene.pereira@cos.uni-heidelberg.de; o.gruss@uni-bonn.de)

Received 26 August 2015; Accepted 9 December 2015

Journal of Cell Science

Journal of Cell Science (2016) 129, 621-636 doi:10.1242/jcs.179713

SSX2IP and PCM1 (Shen and Osmani, 2013; Yukawa et al., 2015). We show that, in contrast to SSX2IP and PCM1, which only associate with cytoplasmic satellite complexes, a large fraction of WDR8 localises to centrioles and basal bodies even when satellites are dispersed. We identified the centriole proximal end protein Cep135 as a WDR8 interactor that recruits WDR8 to centrioles. Strikingly, knockdown of WDR8 blocked the formation of ciliary vesicles at mother centrioles without affecting the localisation of components relevant to ciliation at the distal end of the centriole. WDR8, therefore, represents a new satellite and centriolar protein with ciliary vesicle docking function that is, however, not associated with the site of vesicle docking.

RESULTS

WDR8 is a new SSX2IP-interacting protein

To identify new satellite proteins with functions in ciliogenesis, we searched for interaction partners of SSX2IP by an affinity purification and mass spectrometry approach. We used a murine NIH/3T3 cell line stably expressing human SSX2IP fused to the localisation and purification (LAP) tag (LAP–SSX2IP), under the control of the inducible tetracycline operator (Klinger et al., 2014). LAP–SSX2IP, induced by addition of doxycycline (dox), is known to associate with centriolar satellites in the vicinity of centrosomes in both cycling and ciliated serum-starved NIH/3T3 cells (Klinger et al., 2014). We used LAP–SSX2IP protein complexes under native conditions followed by quantitative mass spectrometry analysis (Boersema et al., 2009; Klinger et al., 2014). We identified endogenous SSX2IP, the known SSX2IP-interacting protein PCM1 (Bärenz et al., 2013; Klinger et al., 2014) and a previously uncharacterised protein named WD repeat containing protein 8 (WDR8), also known as WRAP73 (Fig. 1A; Tables S1 and S2). The interaction between endogenous murine WDR8 and human SSX2IP was confirmed by co-immunoprecipitation assays followed by immunoblotting (Fig. 1B). Likewise, GFP pulldowns from NIH/3T3 cells expressing LAP-tagged human WDR8 (LAP–hWDR8) revealed co-purifying endogenous murine SSX2IP (Fig. 1C). Interestingly, we also found that the *Xenopus laevis* ortholog of human WDR8 (xlWDR8) co-immunoprecipitated with xlSSX2IP (O.G., unpublished data). Thus, WDR8 and SSX2IP are components of conserved protein complexes.

WDR8 localises at centrioles and centriolar satellites

To determine where WDR8, SSX2IP and PCM1 interact, we analysed the subcellular localisation of LAP–hWDR8 in NIH/3T3 cells (Fig. 1D, upper images). LAP–hWDR8 partially colocalised with PCM1 and SSX2IP, yet the satellite colocalisation of WDR8 with SSX2IP was not as prominent as between SSX2IP and PCM1. This suggests that a satellite and a non-satellite fraction of hWDR8 exist. Given that it is known that microtubules organise centriolar satellites (Kubo et al., 1999), we asked whether microtubule depolymerisation with the drug nocodazole disturbs WDR8 localisation. Indeed, colocalisation of WDR8 with the centriolar satellite markers PCM1 and SSX2IP was lost after treatment of NIH/3T3 cells with nocodazole (Fig. 1D, lower images). In addition, we observed two prominent, nocodazole-resistant LAP–hWDR8 signals that overlapped with γ-tubulin (Fig. 1D; Fig. S1). This implies that a pool of WDR8 associates with centrosomes independently of centriolar satellites.

To investigate the localisation of endogenous protein, we raised antibodies against WDR8 in guinea pigs. The antibodies specifically detected exogenous WDR8 in total cell lysates (Fig. S1B,C). This reactivity was largely inhibited by pre-adsorption with the blocking antigen (Fig. S1B,C), indicating specificity to WDR8. In immunofluorescence experiments, the same antibodies recognised endogenous WDR8 at centrosomes and satellites in human retina epithelial (RPE-1) cells (Fig. 1E). The staining was specific to WDR8 given that it markedly decreased upon knockdown of WDR8 using two synthetic small interfering RNAs (siRNAs; Fig. 1F,G, siWDR8_1; siWDR8_2). The localisation of WDR8 was further assessed relative to PCM1 and SSX2IP as well as poly-glutamylated tubulin, which decorates centrioles (Fig. 1E). Similar to NIH/3T3 cells, WDR8 in RPE-1 cells was readily detected at poly-glutamylated-marked centrioles (Fig. 1E). In addition, WDR8 colocalised with a fraction of SSX2IP- and PCM1-stained centriolar satellites (Fig. 1E). Taken together, our data indicate that WDR8 is a centriolar protein that is also present in centriolar satellites.

WDR8 is required for the targeting of centriolar satellite proteins to centrosomes

Colocalisation of WDR8 with SSX2IP and PCM1 at satellites suggests a functional interplay between these proteins at this location. We therefore investigated how depletion of WDR8 affected the localisation of a subset of satellite proteins (Fig. 2). The accumulation of PCM1 (Dammermann and Merdes, 2002), SSX2IP (Bärenz et al., 2013; Hori et al., 2014), Cep290 (Kim et al., 2008) and Cep90 (Kim and Rhee, 2011; Kim et al., 2012) in pericentriolar satellites was apparent in control-depleted cells, but it was considerably diminished upon WDR8 depletion (Fig. 2A–D). Quantification revealed a significant reduction of PCM1, SSX2IP, Cep290 and Cep90 in the vicinity of centrioles in response to WDR8 depletion (Fig. 2E). The steady-state levels of Cep290, PCM1 and SSX2IP were, however, not affected in WDR8-depleted cells (Fig. 2F). Thus, WDR8 influences Cep290, PCM1 or SSX2IP localisation rather than the stability of these proteins. Conversely, downregulation of SSX2IP or PCM1 led to a reduction in the amount of satellite-localised WDR8, implying interdependency in satellite localisation between PCM1, SSX2IP and WDR8 (Fig. S2).

WDR8 is essential for primary cilia formation

Ciliary proteins as well as satellite proteins including SSX2IP, PCM1 and Cep290 are important for proper assembly and function of primary cilia (Craige et al., 2010; Jin et al., 2010; Garcia-Gonzalo et al., 2011; Hori et al., 2014; Klinger et al., 2014). We therefore asked whether WDR8 has a similar role in primary cilia formation. We first analysed the localisation of WDR8 in RPE-1 cells that were grown in low-serum conditions to induce ciliogenesis (Fig. 3A). Cilia were stained with antibodies that recognised poly-glutamylated tubulin, which, together with acetylation, is a tubulin modification enriched at the cilium (Bre et al., 1994) (Fig. 3A). In serum-starved cells, WDR8 colocalised with SSX2IP and PCM1 at centriolar satellites that accumulated around the basal body (i.e. the mother centriole that gave rise to the cilium) (Fig. 3A, 'merged high'). Additionally, WDR8, but not SSX2IP or PCM1, associated with the basal body and the adjacent centriole (Fig. 3A, 'merged low'; see colocalisation with poly-glutamylated tubulin). This indicates that during ciliogenesis WDR8 is a satellite- and basal-body-associated protein.

To investigate the function of WDR8 in cilia formation, we depleted WDR8 in RPE-1 cells prior to serum withdrawal. Both, in control- and WDR8-siRNA-treated cells, the percentage of cells arrested in the G1/G0 phase of the cell cycle upon serum starvation was comparable, as demonstrated by FACS analysis (Fig. S3A).

Journal of Cell Science

Journal of Cell Science (2016) 129, 621-636 doi:10.1242/jcs.179713

A

Cycling cells

Description	MW [kDa]	Unique Pep	Medium/Light	Coverage (%)
Afadin -and a-actinin binding protein (SSX2IP) *homo sapiens*	71.2	20	300.000	61.7
Afadin -and a-actinin binding protein (SSX2IP) *mus musculus*	70.9	13	300.000	48.8
WD repeat containing protein WRAP73 *Mus musculus*	52.0	12	300.000	46.7
Pericentriolar Material 1 protein *Mus musculus*	228.7	44	300.000	33.0

Quiescent cells

Description	MW [kDa]	Unique Pep	Medium/Light	Coverage (%)
Afadin -and a-actinin binding protein (SSX2IP) *homo sapiens*	71.2	10	300.000	31.3
Afadin -and a-actinin binding protein (SSX2IP) *mus musculus*	52.0	6	300.000	15.8
WD repeat containing protein WRAP73 *Mus musculus*	70.9	2	300.000	14.5
Pericentriolar Material 1 protein *Mus musculus*	228.7	11	125.000	6.8

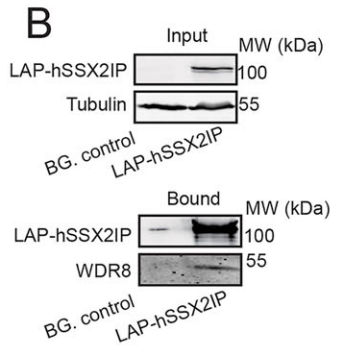

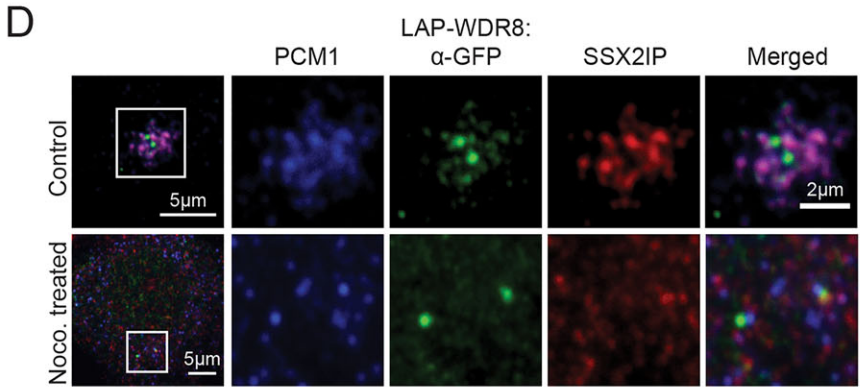

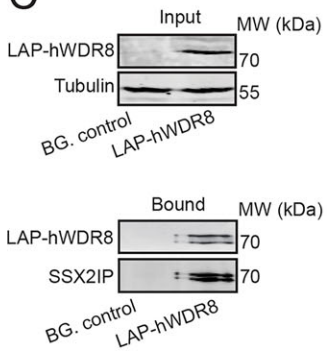

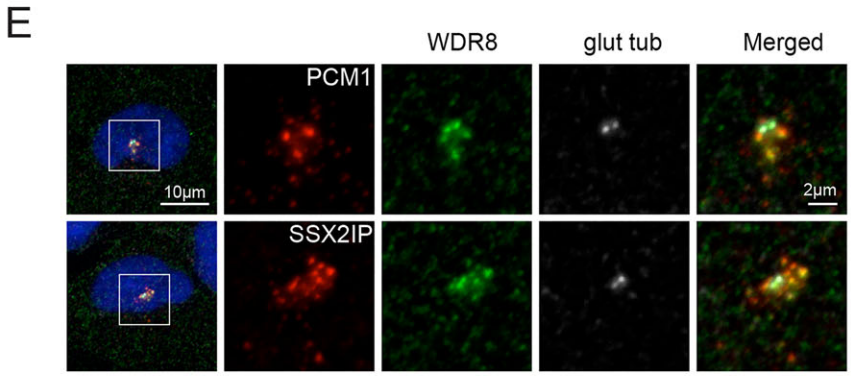

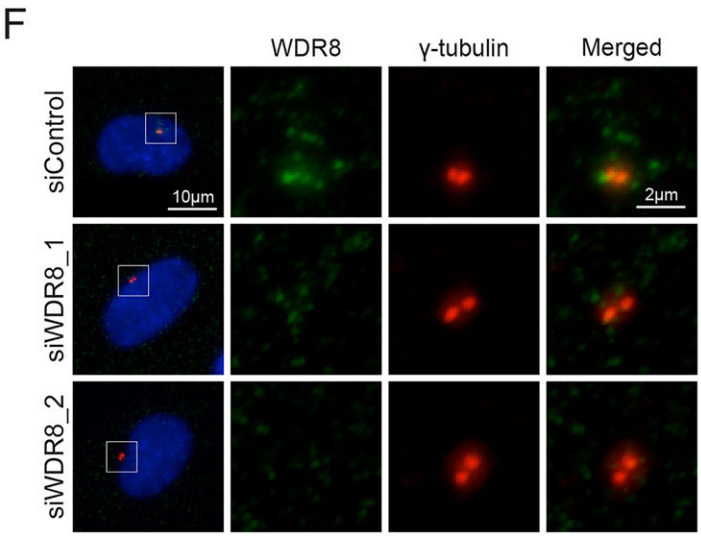

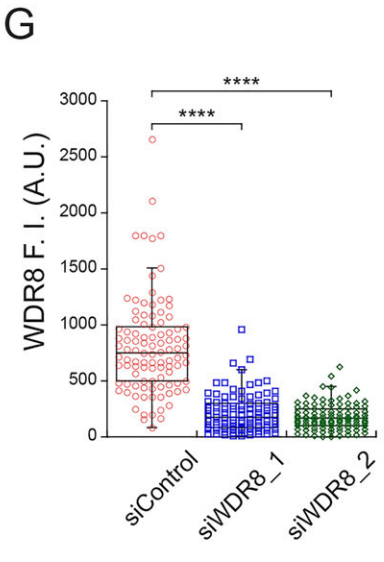

Fig. 1. See next page for legend.

Journal of Cell Science (2016) 129, 621-636 doi:10.1242/jcs.179713

Fig. 1. Identification of WDR8 as a centriolar and centriolar satellite protein in mammalian cells. (A) A list of proteins identified as LAP–SSX2IP interaction partners in NIH/3T3 cells, with name, molecular mass, unique peptides, peptide coverage and the average abundance ratios in LAP–SSX2IP (medium) compared to LAP-only (light) cells (Klinger et al., 2014). A medium-to-light ratio of 300 indicates that the protein was only identified in LAP–SSX2IP cells. (B,C) Lysates from LAP only (background, BG. control), LAP–SSX2IP (B) or LAP–WDR8 (C) cells were used for pulldowns followed by immunoblotting using anti-SSX2IP (B) or anti-WDR8 (C) antibodies. Tubulin served as a loading control. (D) NIH/3T3 cells expressing LAP–SSX2IP were stained with anti-GFP, anti-PCM1 and anti-SSX2IP antibodies before and after microtubule depolymerisation with nocodazole. Enlargements of the indicated areas on the left are shown. (E) Indirect immunofluorescence in RPE-1 cells using antibodies against poly-glutamylated tubulin (glut tub), WDR8, SSX2IP and PCM1. (F) Knockdown of WDR8 with two different siRNAs (siWDR8_1 or siWDR8_2) in RPE-1 cells stained with anti-WDR8 and anti-γ-tubulin antibodies. DNA was stained with DAPI (blue). Enlargements of the areas depicted on the left are shown. (G) Box plots indicate the WDR8 fluorescence intensity as described in the Materials and Methods [fluorescence intensity (F.I.) in arbitrary units (A.U.)] in control- and WDR8-siRNA-treated cells, n=100. ****P<0.001 (Wilcoxon–Mann–Whitney test). The result shown is representative out of four experiments.

However, whereas the majority of control-depleted cells formed a cilium at the mother centriole (stained for Cep164, Fig. 3B), the vast majority of WDR8-depleted cells failed to form a cilium (Fig. 3B,D). The diminished cilia signal upon WDR8 depletion was not an indirect reflection of reduced tubulin glutamylation or acetylation, because the lack of cilia was confirmed with antibodies against the axoneme-associated markers IFT88 and BBS4 (Fig. 3B–D). However, although cilia were absent in WDR8-depleted cells, IFT88 and BBS4 were anchored at the Cep164-stained mother centriole (Fig. 3B,C, arrowheads). This indicates that centrosomal recruitment of IFT88 and BBS4 in response to serum starvation does not require WDR8 function, whereas cilia formation does. Importantly, transient expression of a FLAG-tagged siRNA-resistant version of WDR8 restored primary cilia formation in cells after depletion of endogenous WDR8 (Fig. 3E,F). Collectively, our data show that WDR8 is essential for ciliogenesis.

Removal of CP110–Cep97 from the mother centriole is impaired in the absence of WDR8

Assembly of primary cilia requires removal of the CP110–Cep97 complex from the distal end of the mother centriole to allow growth of axonemal microtubules (Spektor et al., 2007; Tsang et al., 2008). To investigate whether WDR8 is involved in this process, we determined the centriolar association of CP110 and Cep97 in serum-starved control- and WDR8-depleted cells (Fig. 4). As previously reported (Spektor et al., 2007), CP110 and Cep97 localise at the daughter centriole but not at the basal body of ciliated cells (Fig. 4A,B, control). The majority of non-ciliated WDR8-depleted cells maintained CP110 and Cep97 at the basal body and the daughter centriole (Fig. 4A–C). This indicates that WDR8 function is required for CP110–Cep97 removal from the mother centriole during the early steps of ciliogenesis.

We next asked whether the persistence of CP110–Cep97 binding to the basal body is the only cause for the cilia assembly defect in WDR8-depleted RPE-1 cells. To test this hypothesis, we ectopically downregulated CP110 in cells lacking WDR8 (Fig. 4D). The combined treatment of cells with WDR8 and CP110 siRNAs led to a substantial reduction in CP110 at centrioles without affecting centriole binding of IFT88 (Fig. 4D). However, the percentage of cells proficient in primary cilia formation was indistinguishable between WDR8-knockdown and WDR8 and CP110 double-knockdown cells (Fig. 4E). This indicates that WDR8 has at least one more function in ciliogenesis than the displacement of CP110 from the distal end of the mother centriole (basal body).

WDR8 is required for targeting of Rab8 and Arl13b to the basal body

We next asked whether WDR8 could be involved in the establishment of the ciliary vesicle at the mother centriole. This is one of the first steps in ciliogenesis that occurs prior to CP110–Cep97 removal (Das and Guo, 2011; Qin, 2012). To investigate ciliary vesicle formation at the mother centriole, we followed the localisation of the GTPases Arl13b and Rab8a, which are required for ciliary membrane extension at the mother centriole. Upon mock depletion, Arl13b docked to the basal body of cells that started to assemble a cilium (Fig. 5A, top panels) and then decorated the ciliary membrane during axoneme extension (Fig. 5A, middle panel). In contrast, WDR8 depletion almost completely abolished the recruitment of Arl13b to the basal body after serum starvation (Fig. 5A,B). Similar results were obtained with RPE-1 cells stably expressing GFP–Rab8a (Fig. 5C). WDR8 knockdown abolished basal body localisation of Rab8a in 93% of the cells (Fig. 5C,D). We suggest that WDR8 function promotes the docking of Rab8a and Arl13b vesicles to the basal body during ciliogenesis.

It is possible that WDR8 might regulate activation of the GTPase Rab8a. If this hypothesis was correct, one would expect that Rab8a centrosomal localisation and ciliogenesis in WDR8-depleted cells would be rescued by overexpression of a constitutively active GTP-bound form of Rab8a. This hypothesis was tested using RPE-1 cells that stably expressed the hydrolysis-deficient active Rab8a-Q67L mutant protein (Fig. 5E–G). Previously, we have shown that Rab8a-Q67L rescues the ciliogenesis defects of Cep164-depleted cells (Schmidt et al., 2012). However, in WDR8-depleted cells GFP–Rab8a-Q67L failed to localise to basal bodies and did not promote cilia formation (Fig. 5E,F). Therefore, our data indicate that Rab8a activation is not the sole cause of cilia deficiency in cells lacking WDR8.

Vesicle docking at the mother centriole requires WDR8

Next, we used transmission electron microscopy (TEM) to analyse the ultrastructure of the basal body and/or cilia in control and WDR8-knockdown cells. In all control RPE-1 cells (n=12), the distal end of the basal bodies was in contact with the ciliary membrane (Fig. 6A,C). In marked contrast, vesicle docking was absent in nine out of ten basal bodies of WDR8-knockdown cells (Fig. 6B,C). This indicates that vesicle docking to the mother centriole does not take place in the absence of WDR8.

Vesicle docking at the mother centriole requires the presence of distal appendage components, including the proteins Cep164 and Cep123 (Schmidt et al., 2012; Sillibourne et al., 2013; Tanos et al., 2013). As assessed by TEM, distal appendages were present in WDR8-depleted cells (Fig. 6B), indicating that WDR8 is not needed for distal appendage formation. This notion was confirmed by quantitative immunofluorescence microscopy, which indicated that the levels of Cep123 or Cep164 were not reduced in WDR8-depleted cells (Fig. S3B,C). We conclude that WDR8 promotes ciliary vesicle docking at the mother centriole by a mechanism unrelated to formation of distal appendages.

Journal of Cell Science (2016) 129, 621-636 doi:10.1242/jcs.179713

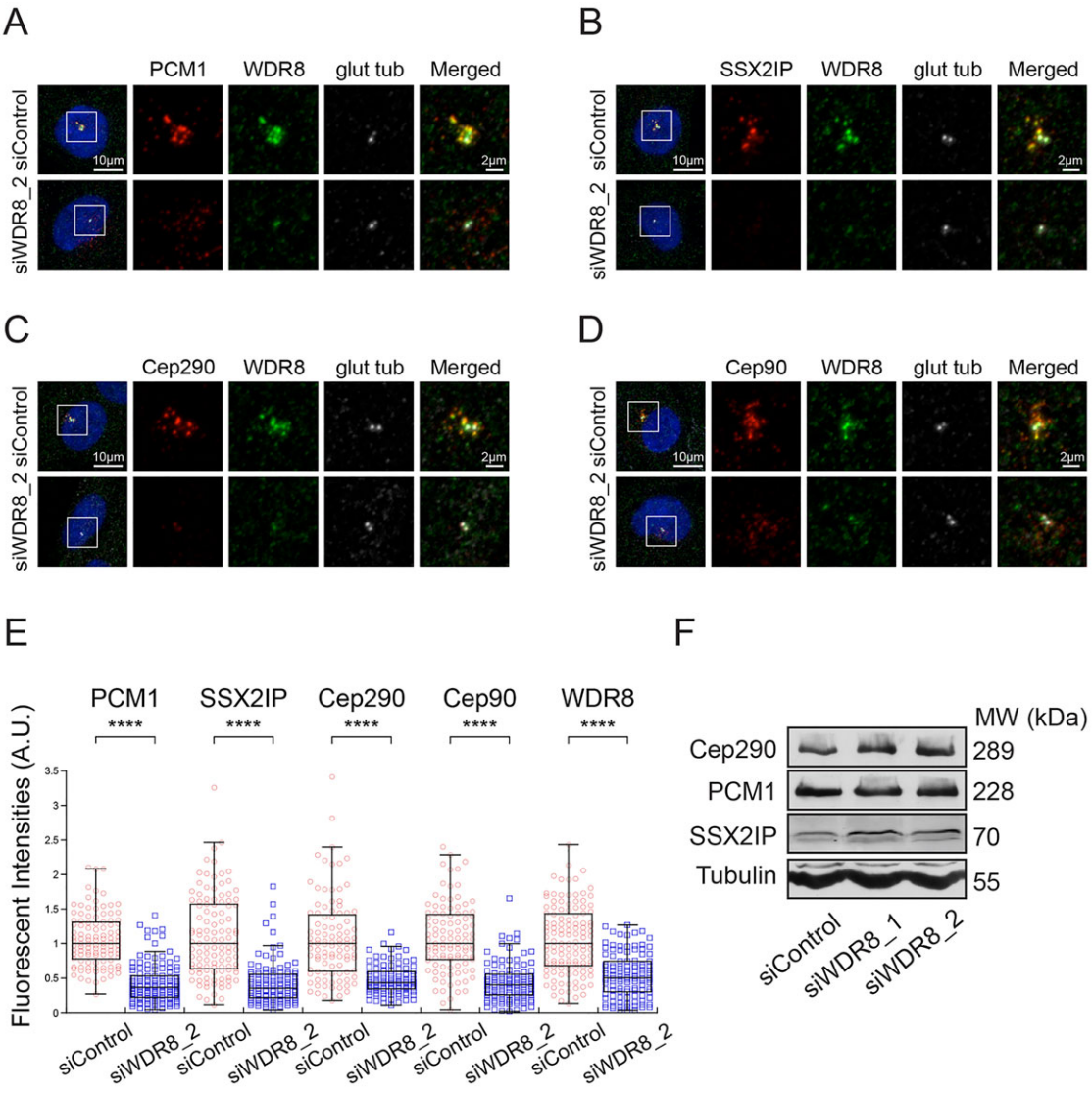

Fig. 2. Role of WDR8 in centriolar satellite organisation. (A) Localisation of PCM1 (A), SSX2IP (B), Cep290 (C) and Cep90 (D) was analysed by indirect immunofluorescence in control- and WDR8-siRNA-treated RPE-1 cells. Poly-glutamylated tubulin (glut tub) served as a centriolar marker. (E) Quantification of the satellite localisation of PCM1, SSX2IP, Cep290, Cep90 and WDR8 (fluorescence intensity) in the encircled area depicted in A to D, *n*=100 cells for each sample. ****$P<0.001$ (Wilcoxon–Mann–Whitney test). Box plots are as described in the Materials and Methods [fluorescence intensity in arbitrary units (A.U.)]. Representative out of three experiments. (D) Immunoblot showing the steady state levels of Cep290, PCM1 and SSX2IP in control- and WDR8-siRNA-treated cells. Tubulin served as a loading control.

Centrosomal localisation of WDR8 depends upon the proximal end protein Cep135

To analyse how WDR8 associates with centrioles, we used murine cell lines stably expressing LAP–hWDR8 to search for WDR8-associated components. In addition to SSX2IP, we found the highly conserved centrosomal proximal end protein Cep135 (Ohta et al., 2002) to be a WDR8 interaction partner in quiescent and cycling cells (Fig. 7A; Tables S3 and S4). Interaction between WDR8 and Cep135 was confirmed by immunoprecipitation experiments using anti-Cep135 antibodies (Fig. 7B). Strikingly, when we compared the centriolar localisation of WDR8 with Cep135 in stimulated emission depletion (STED) and 3D-structured illumination (3D-SIM) microscopy experiments, we observed that LAP–hWDR8 largely colocalised with Cep135 (Fig. 7C, DOX+). The LAP–hWDR8 and Cep135 signals were clearly distinct from the ring-like structure formed by the distal end protein Cep164 (Fig. 7C). Our data thus indicate that Cep135 and WDR8 form a complex at the proximal end of the mother centriole.

To explore the functional relationship between Cep135 and WDR8, we investigated whether Cep135 was required for centrosomal association and/or the function of WDR8 in ciliogenesis. To circumvent the previously described centriole duplication defect that arises from prolonged treatment of cells with Cep135 siRNA (Inanc et al., 2013), we analysed cells in which Cep135 was depleted with siRNA (siCep135_1) for only a short period of time (48 h). Under these conditions, the Cep135 knockdown efficiently reduced Cep135 centrosomal levels without compromising centriole duplication, as inferred by the two side-by-side centrin signals that labelled the two centrioles in G1 cells (Fig. 7D). In cells lacking Cep135, FLAG–WDR8 was absent from centrosomes in the large majority (>99%) of the cells (Fig. 7D). The levels of endogenous WDR8 at centrosomes were significantly decreased upon Cep135 depletion (Fig. 7E,F, EGFP

Journal of Cell Science (2016) 129, 621-636 doi:10.1242/jcs.179713

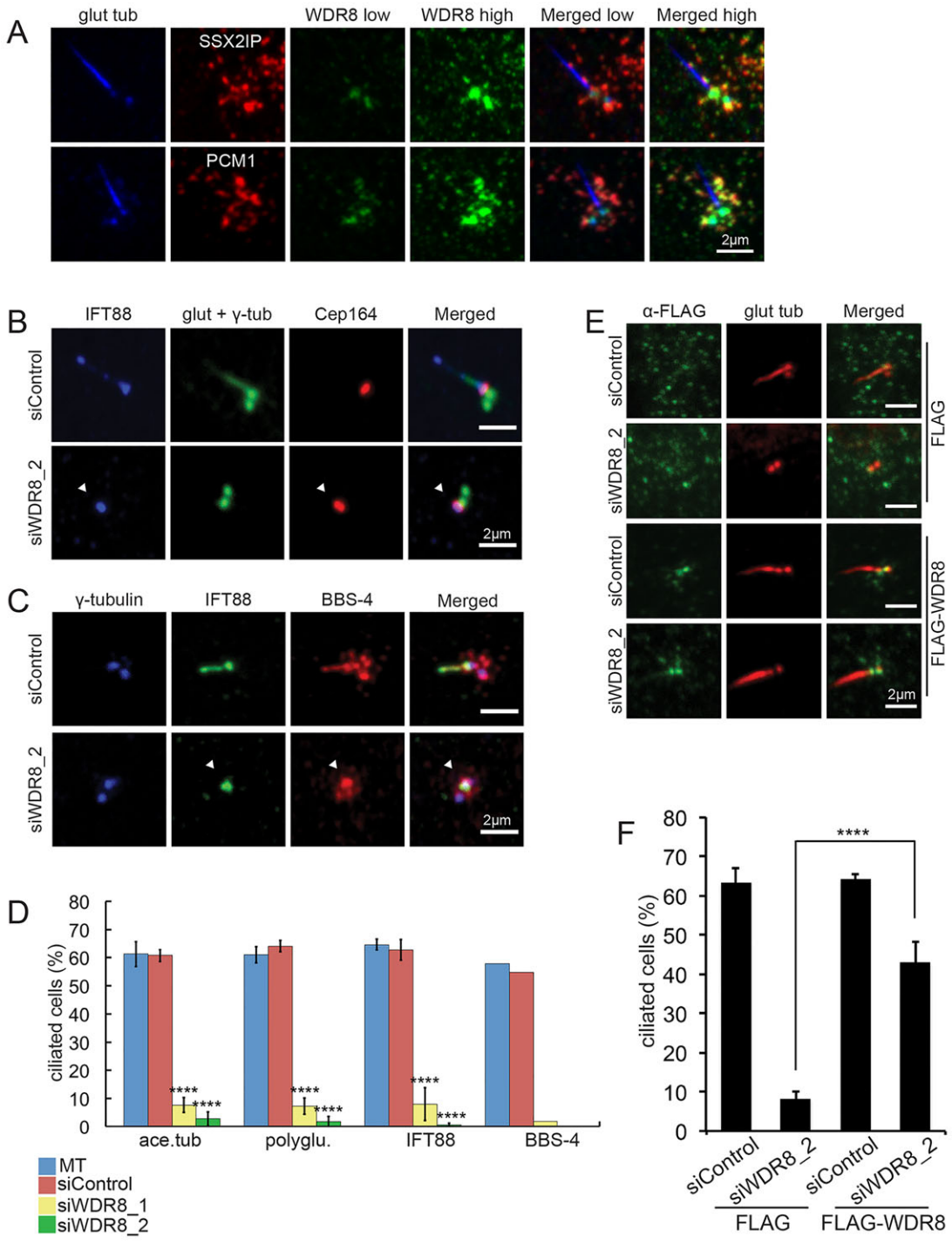

Fig. 3. WDR8 is required for primary cilia formation in RPE-1 cells. (A) Indirect immunofluorescence in ciliated RPE-1 cells using antibodies against poly-glutamylated tubulin (glut tub), WDR8, SSX2IP or PCM1 as indicated. Low and high exposures of the WDR8 signal are shown. (B,C) Immunofluorescence detection of basal body (Cep164), centrioles (γ-tubulin, γ-tub) and the ciliary axonemal marker proteins poly-glutamylated tubulin (glut), IFT88 and BBS-4 in control- and WDR8-siRNA-treated cells as indicated. Arrowheads show centrioles that lack an axoneme. (D) Quantification of the percentage of ciliated cells for experiments described in B and C (the acetylated tubulin staining is not shown in B and C). Three independent experiments were performed for each staining with exception of BBS-4 (n=120 per sample). Results show the mean±s.d. of three independent experiments. ****P<0.001 (t-test). MT, mock treated; ace.tub, acetylated tubulin; polyglu., polyglutamylated tubulin. (E) Analysis of cilia formation in control siRNA (siControl)- and WDR8-siRNA-treated cells transfected with FLAG only or siRNA-resistant FLAG–WDR8 constructs, as indicated. Cilia and centrioles were stained with anti-glutamylated tubulin antibodies (glu tub). FLAG-WDR8 was stained with anti-FLAG antibodies. (F) Quantification of the percentage of ciliated cells for experiments described in E. Error bars show mean±s.d. of three independent experiments (n=120). ****P<0.001 (t-test).

control; Fig. S2D). The expression of a siRNA-resistant rodent (Chinese hamster *Cricetulus griseus*) Cep135 cDNA (CgCep135) (Ohta et al., 2002) in Cep135-depleted cells partly rescued WDR8 localisation at centrioles and, to the same extent, to pericentriolar satellites (Fig. 7E,F). Our data thus indicate that WDR8 is recruited to centrioles in a Cep135-dependent manner.

Journal of Cell Science (2016) 129, 621-636 doi:10.1242/jcs.179713

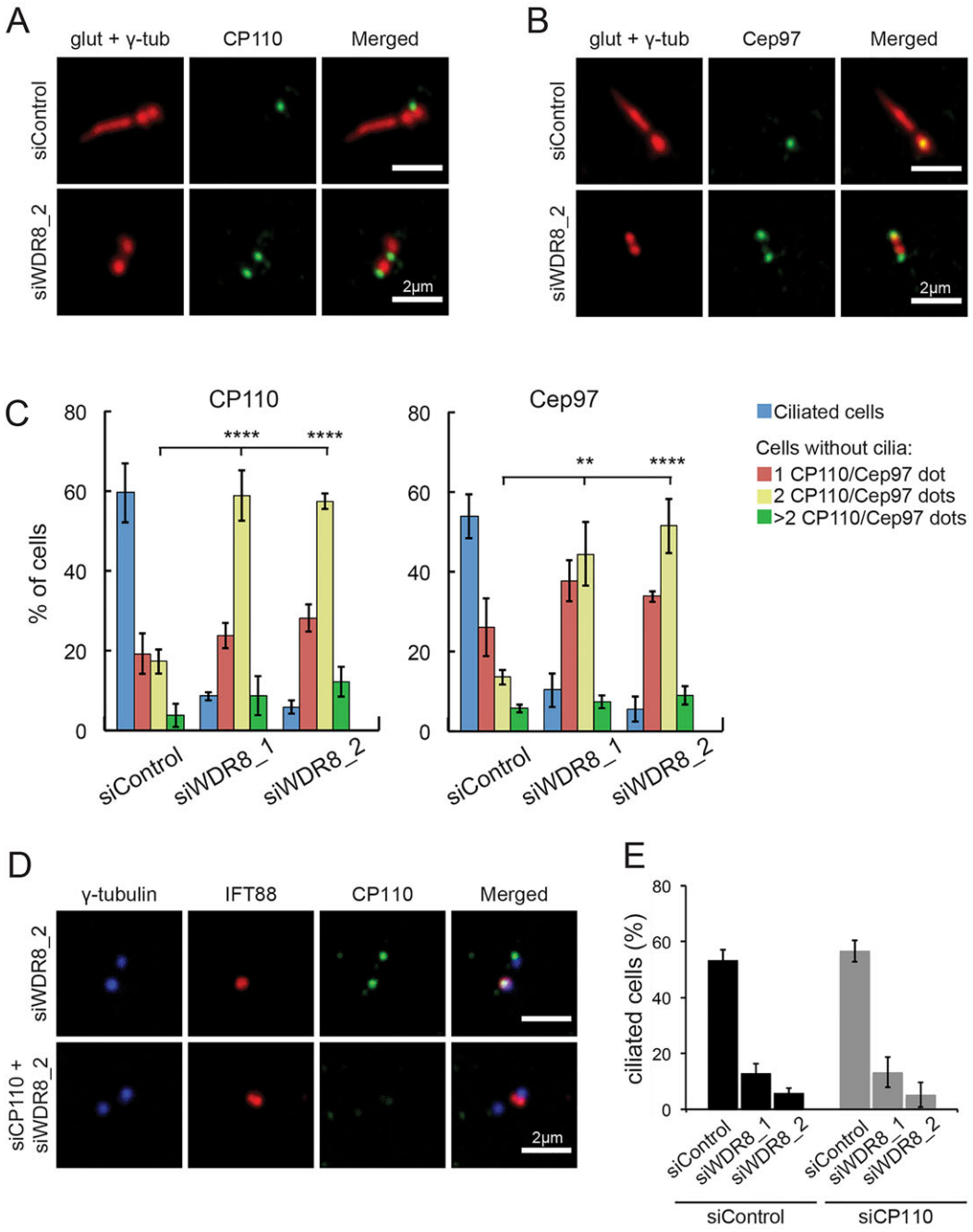

Fig. 4. Knockdown of WDR8 prevents removal of CP110 and Cep97 from mother centrioles. (A,B) Indirect immunofluorescence showing the localisation of CP110 (A) or Cep97 (B) in control- or WDR8-siRNA-treated RPE-1 cells co-stained with antibodies against poly-glutamylated (glut.) and γ-tubulin (γ-tub). (C) Quantification of experiments described in A and B. The percentage of ciliated (blue) and non-ciliated cells with 1 (red), 2 (yellow) or more than 2 (green) CP110 or Cep97 dot-like stainings are indicated. The graphs show mean±s.d. of three independent experiments (n=100 cells per sample). **P<0.01; ****P<0.001 (t-test). (D) RPE-1 cells were treated with WDR8 siRNA alone or in combination with CP110 siRNA and subjected to immunofluorescence analysis with the indicated antibodies. (E) Quantification of experiments described in D. The efficiency of primary cilia formation in WDR8 knockdown, or WDR8 and CP110 double-knockdown cells was quantified based on the IFT88 signal. Results are the mean±s.d. of three independent experiments (n=80 cells per sample).

Cep135 is required for satellite organisation and initiation of ciliogenesis

Considering that the composition of centriolar satellites was strongly dependent on WDR8, we tested whether a similar phenotype would be observed in cells lacking the WDR8 interaction partner Cep135. Short-term knockdown of Cep135 significantly reduced the centrosomal accumulation of Cep290, PCM1 and SSX2IP without compromising centrosome duplication, as judged by the presence of two pericentrin (PCNT)-stained foci (Fig. 8A,B; Fig. S2E). This indicates that Cep135, like WDR8, is required for the targeting of satellite proteins to the centrosome area.

We then investigated whether Cep135 plays a role in ciliogenesis. Under conditions of short-term Cep135 knockdown and serum starvation, primary cilia formation was strongly decreased, as indicated by the lack of staining for the axonemal microtubule markers poly-glutamylated tubulin or IFT88 (Fig. 8C,D). The

Journal of Cell Science (2016) 129, 621-636 doi:10.1242/jcs.179713

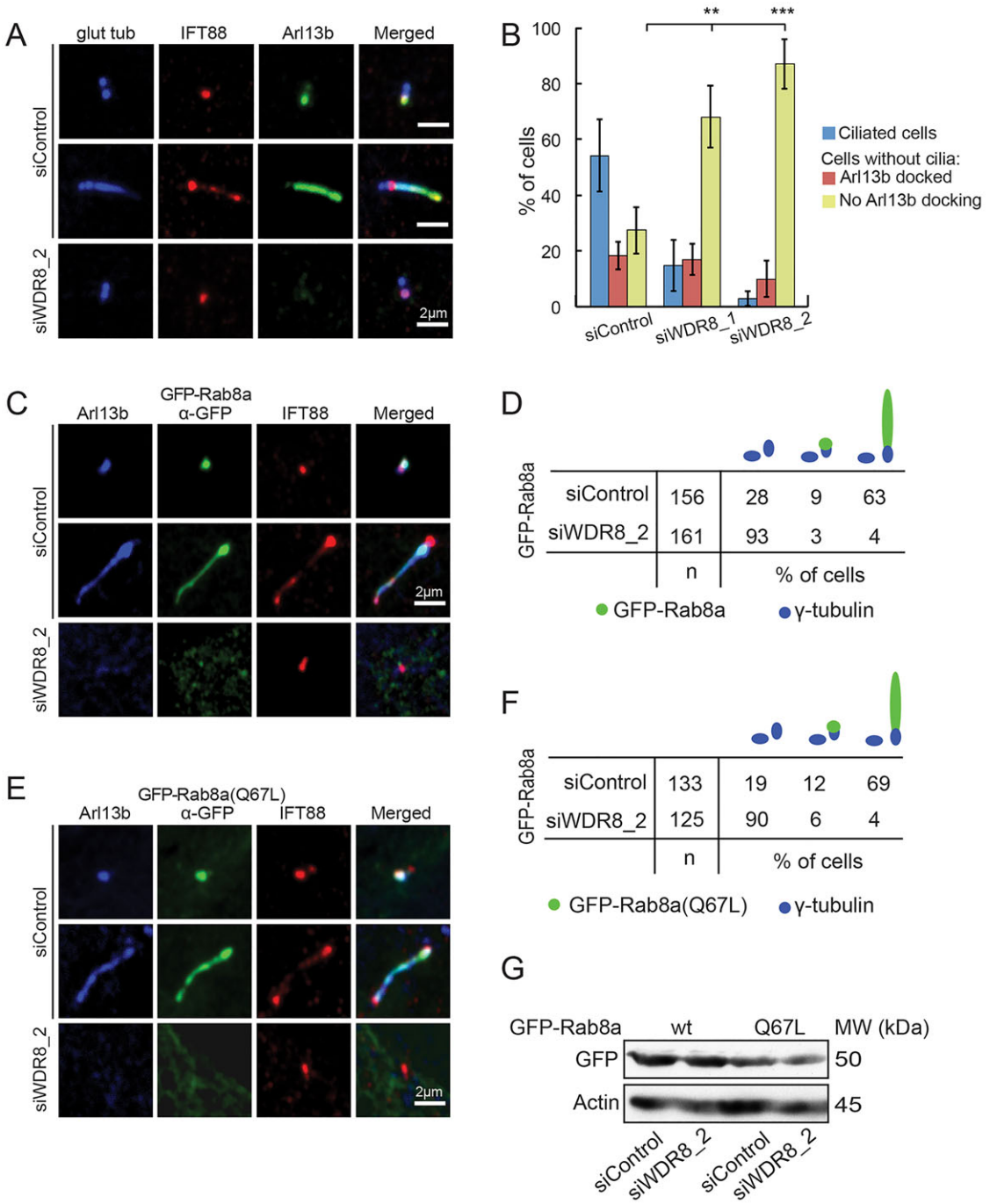

Fig. 5. Knockdown of WDR8 abolishes ciliary membrane docking at centrioles. (A) Poly-glutamylated tubulin (glut tub), IFT88 and the ciliary membrane marker Arl13b were detected in control- or WDR8-siRNA-treated RPE-1 cells by indirect immunofluorescence. (B) Quantification of experiments described in A based on Arl13b staining. Results are the mean±s.d. of three independent experiments (n=100). **P<0.01; ***P<0.005 (t-test). (C–F) Detection of Arl13b and IFT88 in RPE-1 control- or WDR8-siRNA-treated RPE-1 cells stably expressing wild-type GFP–Rab8a (C) or the GTP-hydrolysis-deficient Rab8a-Q67L variant (E). (D,F) Quantification of experiments described in C and E, respectively. The percentage of cells showing axonemal, punctate (i.e. basal body) or only diffuse staining of GFP–Rab8a (D) or GFP–Rab8a-Q67L (F) is depicted. (G) Immunoblot showing the expression levels of GFP–Rab8a and GFP–Rab8a-Q67L in control- and WDR8-siRNA-treated cells. Actin served as a loading control.

diminished ciliogenesis in Cep135-depleted cells was rescued by expression of siRNA-resistant CgCep135 (Fig. 8E,F; Fig. S2D). Despite the lack of cilia, IFT88, as well as the appendage proteins Cep164 and Cep123, were still recruited to centrioles in the absence of Cep135 (Fig. 8C; Fig. S4), resembling WDR8-depleted cells (Fig. 3C). Cep135 depletion affected primary cilia formation almost as strong as WDR8 knockdown (compare Fig. 8D and Fig. 3F). To determine whether Cep135 influenced ciliogenesis in a way similar to WDR8, we analysed the ciliary membrane markers Rab8a and Arl13b. Active GFP–Rab8a (Rab8a-Q67L) and Arl13b accumulated at centrosomes in serum-starved control cells but failed to do so in the majority of Cep135-depleted cells (Fig. 8G,H). Taken together, our data indicate that, similar to WDR8, Cep135 is required for the initial steps of ciliogenesis.

Journal of Cell Science (2016) 129, 621-636 doi:10.1242/jcs.179713

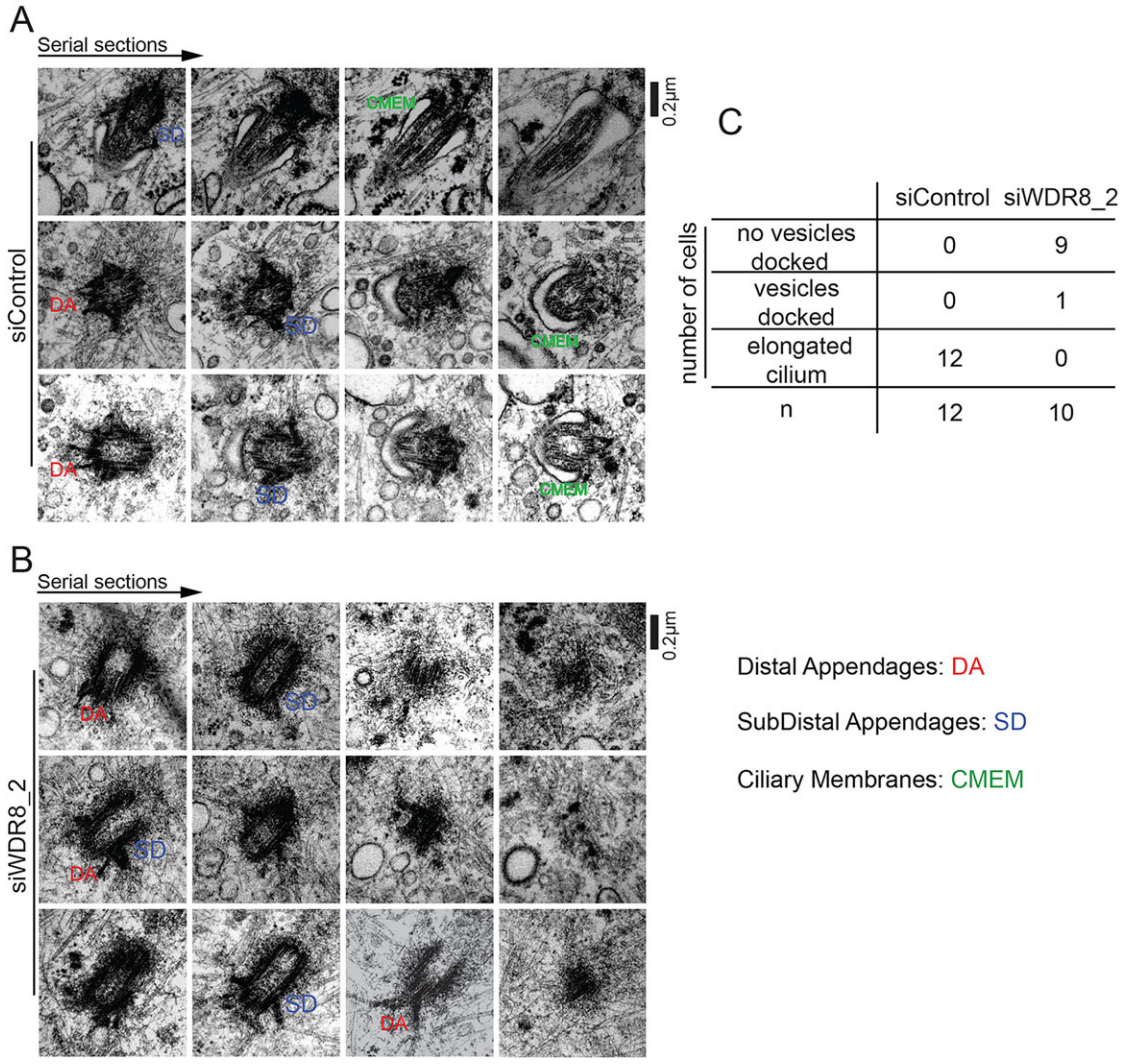

Fig. 6. Electron micrographs of control- and WDR8-siRNA-treated RPE-1 cells. Cells were treated with siControl (A) or siWDR8_2 (B). Each row shows four serial sections of the same centriole. DA (red), distal appendices; SD (blue), subdistal appendices; CMEM (green), ciliary membrane. (C) Quantification of experiments described in A and B.

DISCUSSION

The establishment of the ciliary membrane at the mother centriole is a remarkable process that requires the concerted action of mother centriolar appendage proteins and Golgi-derived vesicular components. Here, we established WDR8 as a centriolar and satellite-associated protein that is indispensable for ciliary vesicle docking at the mother centriole during the early steps of ciliogenesis.

We initially identified WDR8 as a new interaction partner of the previously characterised centriolar satellite protein SSX2IP. WDR8 has also been found to be in complex with SSX2IP in high-throughput mass spectrometry analysis in human cells (Hutchins et al., 2010). Several lines of evidence indicate that WDR8 is a bona fide centriolar satellite component in human and murine cells. Firstly, WDR8 interacts with the satellite components SSX2IP and PCM1. Secondly, endogenous or ectopically expressed fluorescently tagged WDR8 colocalises with SSX2IP and PCM1 in both human and murine cells in the vicinity of centrosomes. Thirdly, WDR8 localisation in satellites, as seen with other satellite protein markers (Kubo et al., 1999), requires an intact microtubule cytoskeleton for centrosome targeting. Finally, targeting of SSX2IP, PCM1 and Cep290 to centrosomes requires WDR8, and vice-versa, indicating interdependency in satellite organisation. Similarly, SSX2IP depletion also affects satellite localisation of PCM1 and Cep290 (Klinger et al., 2014). Thus, the satellite protein network is highly interdependent.

How WDR8 maintains satellite integrity is not clear. Each WD domain of WDR8 consists of 40 amino acids that are regularly involved in mediating protein–protein interactions (Zhang and Zhang, 2015). Six WD repeats are predicted in the human WDR8 primary structure, and, interestingly, we observed that only full-length and not truncated versions of WDR8 were able to co-immunoprecipitate with SSX2IP (our unpublished data). It is therefore possible that the WD repeats of WDR8 have a scaffold and crosslinking function in promoting satellite complex formation and stabilisation.

Importantly, our data indicate that, in contrast to SSX2IP and PCM1, a pool of WDR8 associates with centrioles even when satellites are dispersed. This data is consistent with previous systematic proteomic studies in which WDR8 has been found in

Journal of Cell Science (2016) 129, 621-636 doi:10.1242/jcs.179713

A

quiescent cells

Description	Accession	MW [kDa]	Unique Peptides	Medium/Light	Coverage
WD repeat-containing protein WRAP73 OS=Mus musculus GN=Wrap73	Q9JM98	52.0	7	300.000	21.43
Afadin- and alpha-actinin-binding protein OS=Mus musculus GN=Ssx2ip	Q8VC66	70.9	7	250.000	28.62
Centrosomal protein of 135 kDa OS=Mus musculus GN=Cep135	Q6P5D4	133.3	2	71.482	6.32

cycling cells

Description	Accession	MW [kDa]	Unique Peptides	Medium/Light	Coverage
WD repeat-containing protein WRAP73 OS=Mus musculus GN=Wrap73	Q9JM98	52.0	8	300.000	25.76
Centrosomal protein of 135 kDa OS=Mus musculus GN= Cep135	Q6P5D4	133.3	32	300.000	48.25
Afadin- and alpha-actinin-binding protein OS=Mus musculus GN=Ssx2ip	Q8VC66	70.9	22	300.000	52.54

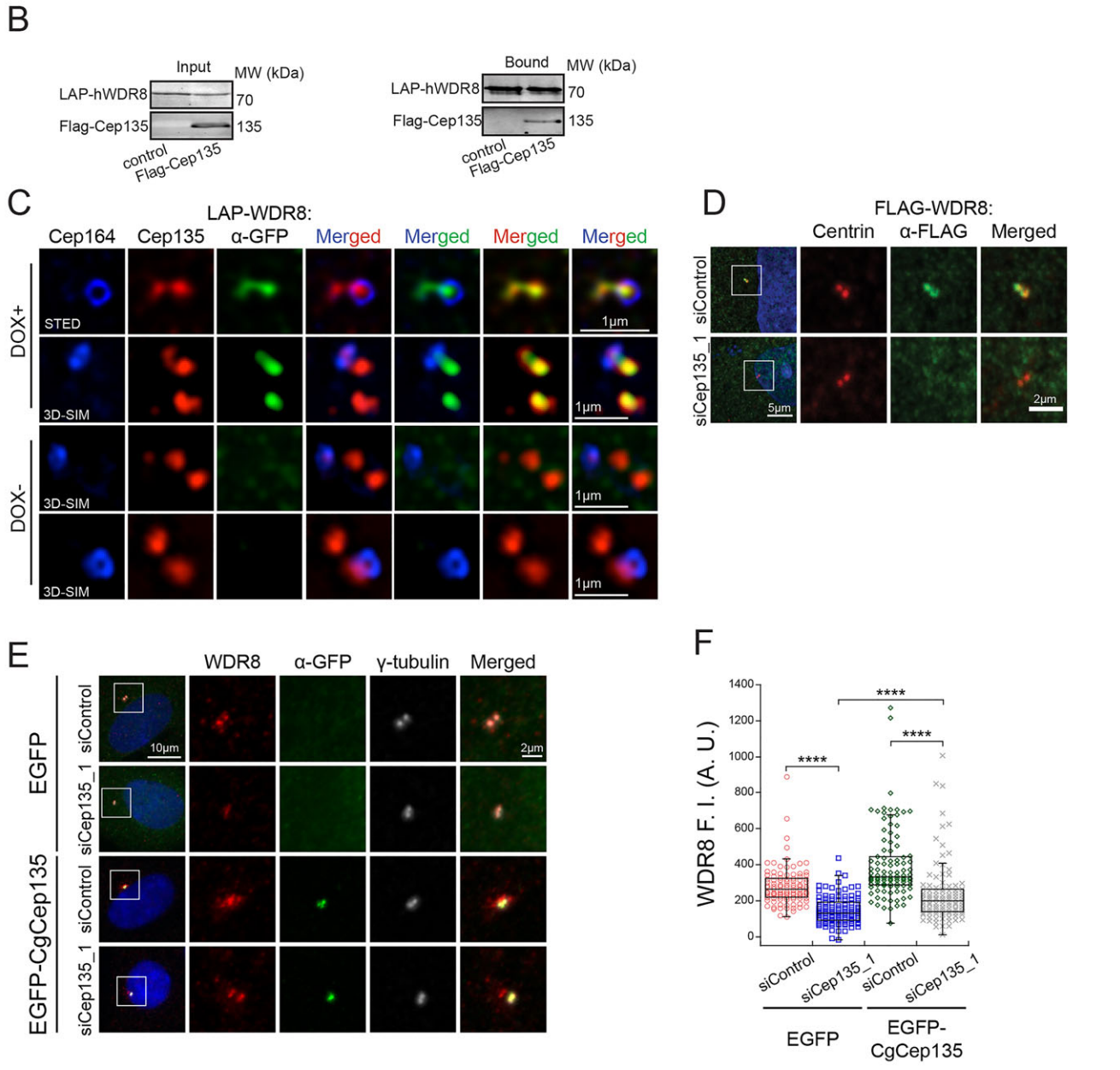

Fig. 7. See next page for legend.

human centrosome fractions (Andersen et al., 2003; Jakobsen et al., 2011). All these findings imply that a pool of WDR8 must tightly associate with centrosomes. The dual localisation at centrioles and satellites is, however, not unique to WDR8, as it has been reported for other satellite proteins such as OFD1 and Cep290, which also localise to centrioles independently of satellites (Tollenaere et al., 2015).

Journal of Cell Science (2016) 129, 621-636 doi:10.1242/jcs.179713

Fig. 7. Identification of WDR8 interaction partners in mammalian cells. Murine NIH/3T3 cells stably expressing LAP–WDR8 were used for purification and identification of WDR8 interaction partners as described in Fig. 1A. Positive WDR8-interacting proteins are listed. (B) LAP only (control) and LAP–WDR8 cells were transfected with FLAG–Cep135 constructs. Pulldowns were performed using GBP beads. Immunoblots were performed with anti-GFP (WDR8) and anti-FLAG (Cep135) antibodies. (C) Colocalisation of Cep164, Cep135 and LAP–WDR8 was determined by super-resolution STED or 3D-SIM microscopy as indicated. Expression of LAP–WDR8 was induced by doxycycline and LAP–WDR8 was detected using anti-GFP antibodies. Cells with (DOX+) or without (DOX–) doxycycline treatment are shown. (D) Analysis of FLAG–WDR8 and centrin localisation by indirect immmunofluorescence in control- and Cep135-siRNA-treated RPE-1 cells. (E) Analysis of WDR8 localisation in control- and Cep135-siRNA-treated cells transfected with EGFP only or siRNA-resistant EGFP–CgCep135 constructs, as indicated. EGFP-CgCep135 was stained with anti-GFP antibodies. Magnifications of the boxed region are shown in the right-hand panels. Blue colour represents nuclear staining by DAPI. (F) Quantification of experiments described in E. Box plots indicate the WDR8 fluorescence intensity as described in the Materials and Methods [fluorescence intensity (F.I.) in arbitrary units (A.U.)], n=100 cells. ****P<0.001 (Wilcoxon–Mann–Whitney test). The result shown is representative out of two independent experiments.

Using WDR8 as a bait, we identified the centrosomal protein Cep135 as a WDR8-binding partner. Short-term depletion of Cep135 almost completely abolished WDR8 centriolar localisation and led to the dispersal of centriolar satellite components, without causing the severe centriole duplication defect and loss of γ-tubulin localisation that has been previously reported for long-term depletion of Cep135 (Inanc et al., 2013). This indicates that Cep135 targets WDR8 to the proximal end of centrioles. Cep135 might also affect the protein stability of WDR8, although difficulty in detecting endogenous WDR8 by immunoblotting prevented us from analysing this possibility in detail. The remarkably similar phenotypes of WDR8 and Cep135 knockdown in ciliogenesis suggest that both proteins share a common function in this process. As Cep135 functions at the proximal end of centrioles (Sonnen et al., 2012; Lin et al., 2013), we suggest that the interacting WDR8 is also associated with the proximal end of the centriole. Our super-resolution data confirmed this hypothesis, as both proteins largely colocalised distantly from the distal end protein Cep164. Interestingly, we sporadically observed a weak Cep135 and LAP–Wdr8 signal closer to the Cep164 ring-like structure. This suggests that low levels of the protein complex could also be present at the distal end of the centriole. Future detailed analysis of endogenous Wdr8 will, however, be necessary to substantiate this conclusion.

Our work establishes that WDR8 plays an essential role in primary cilia biogenesis. The penetrance of cilia loss exceeds the knockdown efficiency indicating that a critical threshold of WDR8 is needed to maintain competence for ciliogenesis. The loss of primary cilia formation upon WDR8 knockdown is considerably more severe than the defect observed upon depletion of SSX2IP (Klinger et al., 2014). SSX2IP-depleted cells are still able to assemble a primary cilium; however, that cilium shows defects in ciliary membrane protein targeting and length (Hori et al., 2014; Klinger et al., 2014). This might suggest that the centriolar WDR8–Cep135 complex plays a more important role in the initiation of cilia biogenesis than the pericentriolar WDR8–SSX2IP complex.

Using fluorescence and electron microscopy, we demonstrate that WDR8 is required for ciliary membrane docking at the mother centriole and displacement of the ciliary inhibitory complex composed of Cep97 and CP110 (which inhibits axoneme extension) (Spektor et al., 2007). Ectopic removal of CP110 did not rescue the cilia biogenesis defect observed upon WDR8 depletion. We thus postulate that the axoneme extension phenotype in WDR8 knockdown cells is most likely a consequence of impaired vesicle docking rather than persistence of the inhibitor Cep97–CP110 protein at the mother centriole per se.

Failure in vesicle docking to distal ends of centrioles has been previously reported for components of distal appendages, such as Cep164 and Cep123, that serve as adaptors for the binding of vesicles to the distal ends (Schmidt et al., 2012; Sillibourne et al., 2013; Tanos et al., 2013; Burke et al., 2014; Joo et al., 2013; Ye et al., 2014). Our data show that WDR8 or Cep135 knockdown does not decrease the centriolar levels of Cep164 or Cep123. This argues against a model in which WDR8 or Cep135 works in ciliary vesicle docking by promoting distal appendage formation, at least not through Cep123 or Cep164.

We propose a model in which Cep135 targets WDR8 to the mother centriole proximal end and this process is required for the initiation of cilia membrane biogenesis that takes place at the distal region of centrioles. In *Drosophila*, depletion of the Cep135 ortholog Bld10 was shown to abolish assembly of the distal central pair of axonemal microtubules in motile cilia (Mottier-Pavie and Megraw, 2009; Carvalho-Santos et al., 2012). Although primary cilia lack the central pair of microtubules, this exemplifies that Cep135 is also required for events that take place at the distal end, i.e. at the site of microtubule polymerisation. It is thus possible that Cep135 and Bld10 might share important functions in cilia formation.

It is currently unclear how loss of WDR8 function causes a block of ciliogenesis at the early stage of vesicle docking. Possibly, loss of WDR8 might abolish targeting of factors required for the function of distal ends in vesicle docking. Such a factor could comprise a yet uncharacterised component of the distal appendage or components that cooperate with the Rab8–Rab11 GTPase cascade in ciliary membrane establishment, such as the recently identified membrane shaping proteins EHD1 and EHD3, and the SNARE component SNAP29 (Lu et al., 2015). Alternatively, the mode of action of WDR8 might involve the targeting of an enzymatic activity, for example, in tubulin modification, to centrioles. The modifying enzyme might localise to the proximal end but generate a diffusible signal that would 'reach' out to the distal ends. Candidates would be kinases, phosphatases or tubulin-modifying enzymes, which could modulate the properties of centriolar microtubules in general.

Interestingly, orthologues of SSX2IP and WDR8 have been found in conserved complexes not only in human cells, as shown here, but previously in *Aspergillus nidulans* (Shen and Osmani, 2013), in *Schizosaccharomyces pombe* (Toya et al., 2007; Yukawa et al., 2015) and *X. laevis* (O.G., unpublished observation). This indicates that the SSX2IP–WDR8 protein module must be highly conserved throughout eukaryotic evolution. In *S. pombe*, the SSX2IP–WDR8 complex functions in interphase and mitosis to anchor microtubules at their minus end in cooperation with the γ-tubulin ring complex (Toya et al., 2007; Yukawa et al., 2015). Consistent with this, SSX2IP has been previously shown to function in primary cilia formation and also in mitosis (Bärenz et al., 2013; Klinger et al., 2014), and we are currently investigating a possible function of WDR8 in mitotic cells. Finally, yeast cells do not rearrange MTOCs for primary cilia formation as in metazoan organisms. The WDR8–SSX2IP module must therefore have acquired an additional function in cells that withdraw from the cell cycle and initiate ciliogenesis. It remains an intriguing question for the future whether a single conserved primary function of the

Journal of Cell Science (2016) 129, 621-636 doi:10.1242/jcs.179713

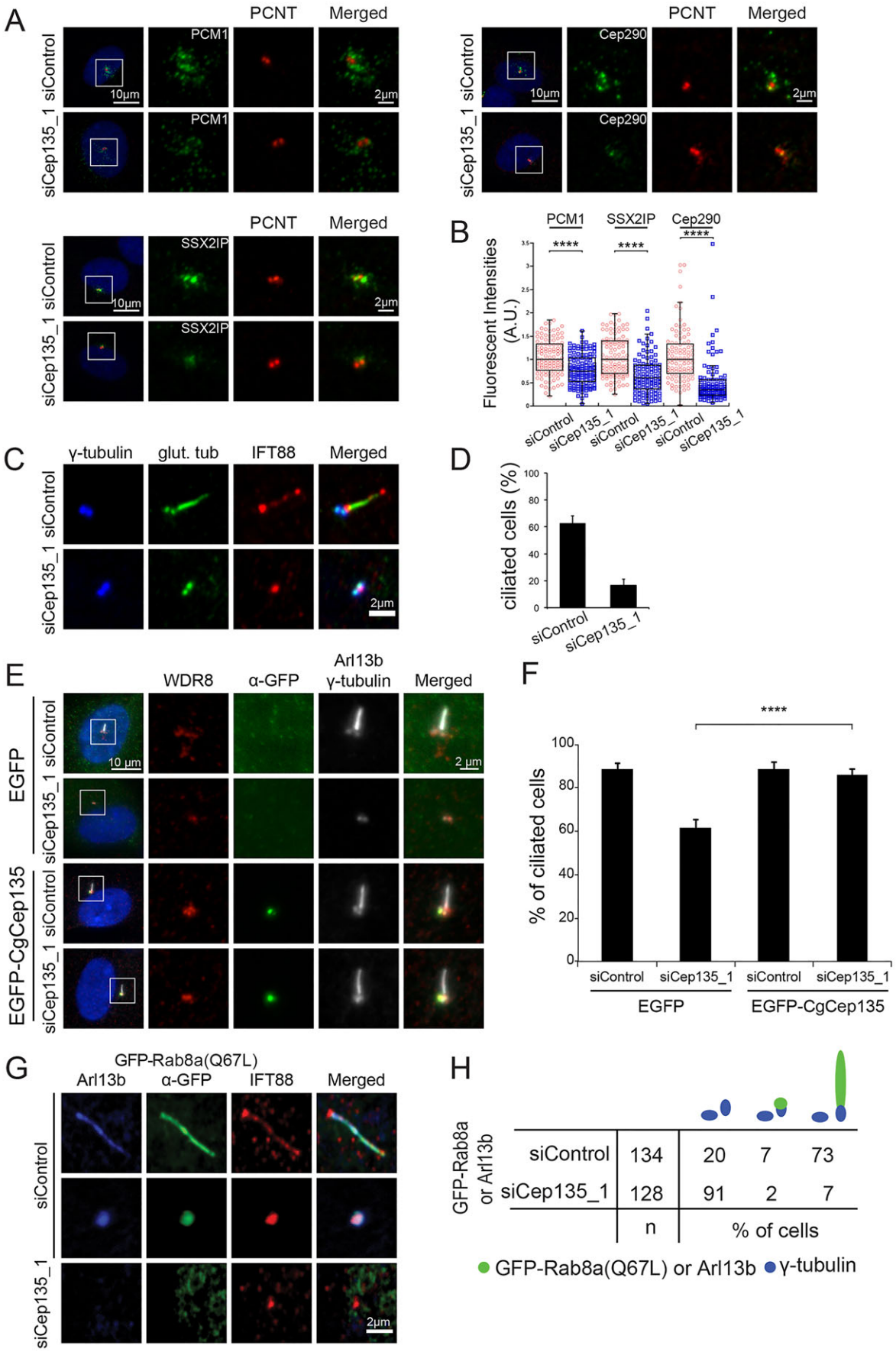

Fig. 8. See next page for legend.

Fig. 8. Centriolar satellite organisation and primary cilia formation in Cep135-depleted cells. (A) Localisation of the centriolar satellite proteins PCM1, SSX2IP and Cep290 in control- and Cep135-siRNA-treated RPE-1 cells. Pericentrin (PCNT) served as a centriolar marker. Blue colour represents nuclear staining by DAPI. (B) Quantification of experiments described in A. The fluorescence intensity was measured in the centrosomal region as depicted in Fig. 2, n=100 cells. ****P<0.001 (Wilcoxon–Mann–Whitney test). The result shown is representative out of two independent experiments. (C) Analysis of primary cilia formation was performed in serum-starved control- and Cep135-siRNA-treated RPE-1 cells. Representative images of immunofluorescence stainings of γ-tubulin, poly-glutamylated tubulin (glut. tub) and IFT88 are shown. (D) Quantification of experiments described in C. Results are the mean±s.d. of a quantification of 130 cells per sample of three independent experiments. (E) Analysis of cilia formation in control- and Cep135-siRNA-treated cells transfected with GFP only or siRNA-resistant CgCep135 constructs, as indicated. Cilia and centrioles were stained with anti-Arl13b and anti-γ-tubulin antibodies, respectively. Blue colour represents nuclear staining by DAPI. (F) Quantification of experiments described in E. Results are the mean±s.d. of three independent experiments, n=100 cells. ****P<0.001 (t-test). (G) Immunofluorescence analysis of Arl13b, GFP–Rab8a and IFT88 localisation in serum-starved control- and Cep135-siRNA-treated RPE-1 cells. (H) Quantification of experiments described in G. The percentage of cells showing axonemal, punctate (i.e. basal body) or only diffuse staining of GFP–Rab8a is indicated. Magnifications of the boxed region are shown in the right-hand panels in A and E.

SSX2IP–WDR8 module explains all the roles of the two individual proteins that have been described throughout the cell cycle.

MATERIALS AND METHODS

Antibodies

Antibodies against human SSX2IP, PCM1 and γ-tubulin were as described previously (Bärenz et al., 2013). Anti-human WDR8 antibodies (1:10) were produced against a recombinant fusion of the N- and C-terminal residues of WDR8 (codons 1–45 and 410–460) purified from *E. coli*. Anti-IFT88 antibodies were raised in rabbit (1:200) and guinea pig (1:250) (against codons 365–824 of mouse IFT88) (Pazour et al., 2002; Gazea et al., 2016). Mouse anti-poly-glutamylated tubulin GT335 (1:1000) was a gift of Carsten Janke (Institute Curie, Paris, France) (Wolff et al., 1992). Rabbit anti-BBS4 antibody (1:250) was a gift from Andrew Fry (University of Leicester, England, UK) (Lopes et al., 2011). Anti-Cep135 (1:100) and anti-pericentrin (1:800) antibodies were gifts from Elmar Schiebel (ZMBH, University of Heidelberg, Germany). Rabbit anti-Cep123 (1:1000) antibody was a gift from Michel Bornens (Institute Curie, Paris, France) (Sillibourne et al., 2013). Rabbit anti-Cep90 (1:200) was a gift of Kunsoo Rhee (Seoul National University, Korea) (Kim and Rhee, 2011). Anti-Cep164 antibodies were generated in rabbits (1:800) and guinea pigs (1:2000) as described previously (Schmidt et al., 2012). For the immunoprecipitation assays, anti-GFP beads were generated using GFP-binding protein (GBP beads) as previously described (Rothbauer et al., 2008; Kuhns et al., 2013).

Antibodies from commercial sources were monoclonal antibodies against GFP (1:800; G1546, Sigma-Aldrich); mouse anti-acetylated tubulin (1:100; sc-23950, Santa Cruz Biotechnology); mouse anti-γ-tubulin (1:500; T6557, Sigma-Aldrich); rabbit anti-γ-tubulin (1:500; T5192; Sigma-Aldrich); rabbit anti-Cep97 and rabbit anti-CP110 (both 1:300; A301-947A and A301-343, Bethyl Laboratories); rabbit anti-Arl13b (1:500; 17711-1-AP, Proteintech); rabbit anti-FLAG antibody (1:500; F7425, Sigma-Aldrich); and rabbit anti-Cep290 (1:1000; A301-659A, Bethyl Laboratories).

Plasmids and reagents

Full-length human WDR8 cDNA (accession number BC086311) was obtained from Source BioScience (Nottingham, UK). Expression constructs comprising N-terminally-tagged YFP, FLAG or LAP were generated in pEYFP-C3 (Takara Bio Inc.), pCMV-3Tag-1A (Agilent Technologies) or pIC113 [LAP construct; a gift from Ian Cheeseman, Whitehead Institute, USA (Cheeseman and Desai, 2005)], respectively. A plasmid carrying Chinese hamster Cep135 cDNA (CgCep135) was a gift of Ryoko Kuriyama (University of Minnesota, USA) (Ohta et al., 2002). Point mutations in WDR8 were generated by site-directed PCR mutagenesis. Expression of TET-on-inducible constructs was induced by the addition of doxycycline (Sigma-Aldrich) at a concentration of 100–1000 ng/ml during serum starvation. For disruption of microtubules, cells were treated with nocodazole (Sigma-Aldrich) at a final concentration of 20 µM for 2 h at 37°C.

Cell culture and transfection

hTERT-immortalised retinal pigment epithelial (RPE-1, ATCC, CRL-4000) cells were grown in DMEM/F12 (Life Technologies) supplemented with 10% fetal calf serum (FCS, Life Technologies), 2 mM L-glutamine and 0.348% sodium bicarbonate. G418 (800 µg/ml, Life Technologies) were added to RPE-1 cells stably expressing GFP–Rab8a. NIH/3T3 cells (ATCC, CRL-1658) were grown in DMEM supplemented with 10% newborn calf serum (NCS, PAN-Biotech). All cell lines were grown at 37°C under 5% CO_2. Transient transfection in NIH/3T3 cells was performed using Lipofectamine 2000 (Life Technologies) according to the manufacturer's protocol. RPE-1 cells were transiently transfected with plasmid DNA by electroporation using the Neon® Transfection System (Life Technologies) according to the manufacturer's protocol. Stable NIH/3T3 cells were generated as previously described (Kuhns et al., 2013). NIH/3T3 and RPE-1 cells were incubated in serum-free medium for 24–48 h to induce ciliogenesis. At least 100 cells were counted for the quantification of ciliated cells for each experimental condition. HEK293T (ATCC CRL-1573) cells were cultured in DMEM supplemented with 10% FCS and transfected with the calcium phosphate precipitation method. All cell lines were authenticated by Multiplex Cell line Authentication (MCA) and were tested for contamination by Multiplex cell Contamination Testing (McCT) v.2 service provided by Multiplexion (Heidelberg, Germany).

RNAi

Transfections of the siRNAs were performed using Lipofectamine RNAiMAX reagent (Life Technologies). The following siRNAs (20 nM, silencer select, Life Technologies) were used: WDR8_1: 5′-GGAAUUC-CAUCUGCGGAUA-3′, WDR8_2: 5′-CCAAGAUAGUGGUGUAUAA-3′; SSX2IP_1: 5′-GGAAGGUUGCUAUAGUGGA-3′, SSX2IP_2: 5′-GC-AUGUCUAAACUUACUAA-3′; Cep135_1: 5′-GAUCUAGAGAAAUC-GCUUU-3′, CEP135_2: 5′-GCAAAUUGAUGAACCGGUU-3′ CP110: 5′-AAGCAGCATGAGTATGCCAGT-3′ (Spektor et al., 2007). Unless otherwise indicated, after 24 h of knockdown, RPE-1 cells were incubated in serum-free medium for 48 h to induce ciliogenesis.

Protein extraction and immunoblotting

For preparation of cell lysates, cells were washed in pre-warmed PBS and re-suspended in 0.8 ml of PBS containing 0.15 ml of 1.85 M NaOH. Cells were kept on ice for 5 min before addition of 0.15 ml of 55% trichloroacetic acid (TCA; w/w). After an incubation of 10 min on ice, samples were centrifuged at 20,800 ***g*** for 15 min at 4°C. The pellet was resuspended in HU-DTT buffer (8 M urea, 0.2 M Tris-HCl pH 6.8, 5% SDS, Bromophenol Blue and 0.1 M DTT), heated for 15 min at 65°C and loaded onto SDS-PAGE gels. Proteins were transferred onto nitrocellulose membranes using a semi-dry blotter. Immunoblotting was carried out using anti-WDR8, anti-FLAG and anti-GFP antibodies. Affinity purified anti-WDR8 antibodies, pre-adsorbed with purified WDR8 antigen, were used in the experiments shown in Fig. S1B,C.

Co-immunoprecipitation and mass spectrometry

Co-immunoprecipitaion in NIH/3T3 LAP–hSSX2IP cells was carried out as described previously (Cheeseman and Desai, 2005; Klinger et al., 2014) with immobilised GBP beads. In brief, NIH/3T3 LAP–hSSX2IP cells were induced with 1 µg/ml doxycycline for 24 h. Cells were either incubated in serum-rich medium (cycling cultures) or serum starved for a total of 48 h to induce ciliogenesis. Cells were lysed and incubated for 3 h at 4°C with GBP beads and processed as described previously (Kuhns et al., 2013). Bound proteins were analysed by SDS-PAGE and immunoblotting. For quantitative mass spectrometry analysis, comparison of negative control and LAP–hSSX2IP pulldown samples was performed after dimethyl labelling using stable isotopes (Boersema et al., 2009). Proteins, separated by SDS-PAGE

Journal of Cell Science (2016) 129, 621-636 doi:10.1242/jcs.179713

and stained with Coomassie Blue, were digested with trypsin as described previously (Bärenz et al., 2013) except that triethylammoniumbicarbonate buffer (TEAB) was used instead of ammoniumbicarbonate buffer. Following digestion, tryptic peptides were extracted from the gel pieces with 50% acetonitrile and 0.1% trifluoroacetic acid (TFA) and concentrated nearly to dryness in a speedVac vacuum centrifuge. As previously described (Boersema et al., 2009), dimethyl labelling was performed by incubating samples with 20 µl 50 mM phosphate buffer pH 7.5, 4 µl 150 mM $NaBH_3CN$ and 4 µl 1% formaldehyde ('light' or 'medium') for 1 h at 25°C. The 'light' and 'medium' labelled samples were loaded separately on a C18 trapping column with a flow rate of 10 µl/min of 0.1% TFA and thereby mixed. Peptides were subsequently separated on an analytical column (75 µm×150 mm) with a flow rate of 300 nl/min coupled to a ESI LTQ Orbitrap XL MS (Thermo Fisher, USA). One survey scan (resolution: 60,000) was followed by five information-dependent product ion scans in the LTQ. Only double- and triple-charged ions were selected for fragmentation. Data were analysed using Proteome Discoverer 1.4 and Mascot (Matrix Science; version 2.4). Mascot was set up to search the SwissProt database, taxonomy *Mus* (16,700 entries) using trypsin as protease, a fragment ion mass tolerance of 0.50 Da and a parent mass tolerance of 4.0 ppm. Iodoacetamide derivative of cysteine was specified in Mascot as a fixed modification. Deamidation of asparagine and oxidation of methionine were specified in Mascot as variable modifications. The target decoy PSM validator was set to a target FDR (strict) of 0.01.

Indirect immunofluorescence and microscopy

Cells were grown on coverslips and fixed in ice-cold methanol at −20°C for 5 min. Cells were blocked with PBS containing 10% FCS and 0.2% Triton X-100 (blocking buffer) for 60 min and incubated with primary antibodies at room temperature for 1 h. The cells were incubated with Alexa-Fluor-488-, 568- or 633-conjugated secondary antibodies (Life Technologies) for 1 h at room temperature. All antibodies were diluted in blocking solution. Coverslips were mounted on glass slides in Mowiol (EMD Millipore) containing 4′,6-diamidino-2-phenylindole (DAPI). Images were acquired as *z*-stacks using the Zeiss LSM780 (Carl Zeiss, Oberkochen, Germany) confocal system and software (ZEN2) or using a Zeiss Axio Observer inverted microscope with a Plan-APOCHROMAT 63×1.4 NA oil objective.

For 3D-SIM, NIH/3T3 cells stably expressing LAP–WDR8 were treated with 1 µg/ml doxycycline for 18 h and with 5 µg/ml of nocodazole for 2 h to disperse the satellite pool of WDR8. Cells were processed for immunofluorescence microscopy as described above, except that secondary antibodies were coupled to Alexa Fluor 488, 555 or 647 (Molecular Probes). Cells were mounted in Prolong Gold antifade reagent (Molecular Probes). Samples were analysed with 3D-SIM Nikon Ti inverted microscope equipped with three lasers (488, 561 and 640 nm), a Nikon Apo TIRF 100×1.49 NA oil immersion objective and an Andor iXon3 DU-897E single-photon detection EMCCD camera. After image capturing, raw images were reconstructed in the NIS-Elements program of the microscope to obtain 3D-SIM images.

STED microscopy was performed on a Leica TCS SP8 STED 3X confocal laser scanning microscope using a HC PL APO 100×1.40 NA oil STED WHITE objective. Images of single confocal sections were taken and processed using the Leica LAS X Core software with STED and deconvolution algorithms.

Images were processed in ImageJ, Photoshop CS3 (Adobe) and Illustrator CS3 (Adobe). No manipulations were performed other than brightness, contrast and colour balance adjustments. Rolling ball background subtractions (ImageJ) were performed in Figs 1E,F, 2A–D, 7E and 8A,E.

Fluorescence intensity measurement

Quantification of fluorescence intensity was performed using original confocal images and the ImageJ 1.47T software (National Institutes of Health, Bethesda, MA). Measurement of integrated density was performed using the summed projections of acquired *z*-stacks in the areas indicated in the figures. γ-tubulin was used as a marker of the centrosome. The centrosome area was defined by a circle of 2-µm diameter and the centriolar satellite region by a circle of 5-µm diameter around γ-tubulin. The data were plotted as box plots using KaleidaGraph 4.0 (Synergy Software). Boxes showing the lower and upper quartiles represent the data value located halfway between the median and the smallest and largest data values, respectively. Outliers are the points whose value is either greater than the upper quartile value plus 1.5 times the interquartile difference or less than lower quartile value minus 1.5 times interquartile difference. Statistical analyses of fluorescence intensity measurements and ciliation assays were performed as specified in figure legends.

Rescue experiments

For rescue experiments, the plasmid containing FLAG-tagged human WDR8 was changed into an siRNA-resistant version using site-directed mutagenesis. The rescue construct (WDR8 siRNA_2 resistant or EGFP–CgCep135) or control vector (FLAG or EGFP) was transiently transfected into RPE-1 cells 2 h prior to the transfection of the cells with control siRNA (siControl) or siWDR8_2. After 24 h, cells were serum starved for 24 h, fixed and processed for immunofluorescence analysis. Approx. 100 cells were counted for each experimental condition.

Transmission electron microscopy

Electron microscopy was performed as previously described (Kuhns et al., 2013; Schmidt et al., 2012). In brief, RPE-1 cells growing on coverslips were fixed with 2.5% glutaraldehyde, washed with 50 mM cacodylate buffer and postfixed in 2% OsO_4 at 4°C. Cells were incubated in 0.5% aqueous uranyl acetate overnight and dehydrated at 4°C using ascending ethanol concentrations and propylene oxide. Cells were incubated in a 1:1 mixture of Epon and propylene oxide, infiltrated with Epon and polymerised at 60°C. Serial ultrathin sections (70 nm) were produced and poststained with uranyl acetate and lead citrate. The stained samples were examined under a transmission electron microscope (EM 910; Carl Zeiss, Oberkochen, Germany). The brightness and contrast of the images were adjusted in Photoshop CS3 (Adobe).

Acknowledgements

We would like to thank Carsten Janke, Michel Bornens, Elmar Schiebel, Ian Cheeseman, Andrew Fry, Ryoko Kuriyama and Kunsoo Rhee for sharing reagents; Laurence Pelletier for exchange of data prior to publication; the mass spectrometry core facilities of the ZMBH for protein identification; the electron microscopy facility of the DKFZ for help with the imaging of electron microscopy samples and the microscopy facilities of the DKFZ, ZMBH and Heidelberg-University Nikon Imaging Center for providing access to microscopes, help with imaging and image processing. We are grateful to Leica Microsystems, Mannheim, Germany for allowing access to the Leica SP8 STED 3X microscope unit. W.W. was a PhD student of the Hartmut Hoffmann-Berling International Graduate School for Molecular and Cellular Biology (HBIGS), University of Heidelberg, Germany.

Competing interests

The authors declare no competing or financial interests.

Author contributions

O.G. and G.P. designed the study and wrote the manuscript. B.K. and W.W. performed most of the experiments. B.C. performed super-resolution analysis (SIM), L.V. helped with the analysis of appendage proteins in Cep135-depleted cells, R.D.S. tested the specificity of anti-WDR8 antibodies, T.R. did the mass spectrometry analysis, and A.N. prepared the samples for electron microscopy and helped with the imaging analysis. All authors edited the manuscript.

Funding

This work was funded as a German Cancer Research Centre (DKFZ) and Zentrum für Molekulare Biologie der Universität Heidelberg (ZMBH) alliance bridging project within the German excellence initiative (ZUK49) awarded to the Heidelberg University (to G.P. and O.J.G.); O.J.G. was supported in part by a start-professorship [ZUK 49/TP1-16]; B.K., L.V. and B.C. are members of The Hartmut Hoffmann-Berling International Graduate School of Molecular and Cellular Biology (HBIGS). B.K. and L.V. are supported by the German Research Council (DFG) cooperative research grant [project number A14, SFB873 to G.P.]; G.P. is supported by the Heisenberg Program of the DFG [number PE1883-2].

Supplementary information

Supplementary information available online at
http://jcs.biologists.org/lookup/suppl/doi:10.1242/jcs.179713/-/DC1

References

Andersen, J. S., Wilkinson, C. J., Mayor, T., Mortensen, P., Nigg, E. A. and Mann, M. (2003). Proteomic characterization of the human centrosome by protein correlation profiling. *Nature* **426**, 570-574.

Badano, J. L., Mitsuma, N., Beales, P. L. and Katsanis, N. (2006). The ciliopathies: an emerging class of human genetic disorders. *Annu. Rev. Genomics Hum. Genet.* **7**, 125-148.

Baker, K. and Beales, P. L. (2009). Making sense of cilia in disease: the human ciliopathies. *Am. J. Med. Genet. C Semin. Med. Genet.* **151C**, 281-295.

Bärenz, F., Mayilo, D. and Gruss, O. J. (2011). Centriolar satellites: busy orbits around the centrosome. *Eur. J. Cell. Biol.* **90**, 983-989.

Bärenz, F., Inoue, D., Yokoyama, H., Tegha-Dunghu, J., Freiss, S., Draeger, S., Mayilo, D., Cado, I., Merker, S., Klinger, M. et al. (2013). The centriolar satellite protein SSX2IP promotes centrosome maturation. *J. Cell Biol.* **202**, 81-95.

Boersema, P. J., Raijmakers, R., Lemeer, S., Mohammed, S. and Heck, A. J. R. (2009). Multiplex peptide stable isotope dimethyl labeling for quantitative proteomics. *Nat. Protoc.* **4**, 484-494.

Bre, M. H., de Nechaud, B., Wolff, A. and Fleury, A. (1994). Glutamylated tubulin probed in ciliates with the monoclonal antibody GT335. *Cell Motil. Cytoskeleton* **27**, 337-349.

Burke, M. C., Li, F.-Q., Cyge, B., Arashiro, T., Brechbuhl, H. M., Chen, X., Siller, S. S., Weiss, M. A., O'Connell, C. B., Love, D. et al. (2014). Chibby promotes ciliary vesicle formation and basal body docking during airway cell differentiation. *J. Cell Biol.* **207**, 123-137.

Carvalho-Santos, Z., Machado, P., Alvarez-Martins, I., Gouveia, S. M., Jana, S. C., Duarte, P., Amado, T., Branco, P., Freitas, M. C., Silva, S. T. N. et al. (2012). BLD10/CEP135 is a microtubule-associated protein that controls the formation of the flagellum central microtubule pair. *Dev. Cell* **23**, 412-424.

Cheeseman, I. M. and Desai, A. (2005). A combined approach for the localization and tandem affinity purification of protein complexes from metazoans. *Sci. STKE* **2005**, pl1.

Craige, B., Tsao, C.-C., Diener, D. R., Hou, Y., Lechtreck, K.-F., Rosenbaum, J. L. and Witman, G. B. (2010). CEP290 tethers flagellar transition zone microtubules to the membrane and regulates flagellar protein content. *J. Cell Biol.* **190**, 927-940.

Dammermann, A. and Merdes, A. (2002). Assembly of centrosomal proteins and microtubule organization depends on PCM-1. *J. Cell Biol.* **159**, 255-266.

Das, A. and Guo, W. (2011). Rabs and the exocyst in ciliogenesis, tubulogenesis and beyond. *Trends Cell Biol.* **21**, 383-386.

Fliegauf, M., Benzing, T. and Omran, H. (2007). When cilia go bad: cilia defects and ciliopathies. *Nat. Rev. Mol. Cell Biol.* **8**, 880-893.

Garcia-Gonzalo, F. R., Corbit, K. C., Sirerol-Piquer, M. S., Ramaswami, G., Otto, E. A., Noriega, T. R., Seol, A. D., Robinson, J. F., Bennett, C. L., Josifova, D. J. et al. (2011). A transition zone complex regulates mammalian ciliogenesis and ciliary membrane composition. *Nat. Genet.* **43**, 776-784.

Gazea, M., Tasouri, E., Tolve, M., Bosch, V., Kabanova, A., Gojak, C., Kurtulmus, B., Novikov, O., Spatz, J., Pereira, G. et al. (2016). Primary cilia are critical for Sonic hedgehog-mediated dopaminergic neurogenesis in the embryonic midbrain. *Dev. Biol.* **409**, 55-71.

Hori, A., Ikebe, C., Tada, M. and Toda, T. (2014). Msd1/SSX2IP-dependent microtubule anchorage ensures spindle orientation and primary cilia formation. *EMBO Rep.* **15**, 175-184.

Hutchins, J. R. A., Toyoda, Y., Hegemann, B., Poser, I., Heriche, J. K., Sykora, M. M., Augsburg, M., Hudecz, O., Buschhorn, B. A., Bulkescher, J. et al. (2010). Systematic analysis of human protein complexes identifies chromosome segregation proteins. *Science* **328**, 593-599.

Inanc, B., Putz, M., Lalor, P., Dockery, P., Kuriyama, R., Gergely, F. and Morrison, C. G. (2013). Abnormal centrosomal structure and duplication in Cep135-deficient vertebrate cells. *Mol. Biol. Cell* **24**, 2645-2654.

Ishikawa, H. and Marshall, W. F. (2011). Ciliogenesis: building the cell's antenna. *Nat. Rev. Mol. Cell Biol.* **12**, 222-234.

Jakobsen, L., Vanselow, K., Skogs, M., Toyoda, Y., Lundberg, E., Poser, I., Falkenby, L. G., Bennetzen, M., Westendorf, J., Nigg, E. A. et al. (2011). Novel asymmetrically localizing components of human centrosomes identified by complementary proteomics methods. *EMBO J.* **30**, 1520-1535.

Jin, H., White, S. R., Shida, T., Schulz, S., Aguiar, M., Gygi, S. P., Bazan, J. F. and Nachury, M. V. (2010). The conserved Bardet-Biedl syndrome proteins assemble a coat that traffics membrane proteins to cilia. *Cell* **141**, 1208-1219.

Joo, K., Kim, C. G., Lee, M.-S., Moon, H.-Y., Lee, S.-H., Kim, M. J., Kweon, H.-S., Park, W.-Y., Kim, C.-H., Gleeson, J. G. et al. (2013). CCDC41 is required for ciliary vesicle docking to the mother centriole. *Proc. Natl. Acad. Sci. USA* **110**, 5987-5992.

Kim, S. and Dynlacht, B. D. (2013). Assembling a primary cilium. *Curr. Opin. Cell Biol.* **25**, 506-511.

Kim, K. and Rhee, K. (2011). The pericentriolar satellite protein CEP90 is crucial for integrity of the mitotic spindle pole. *J. Cell Sci.* **124**, 338-347.

Kim, J., Krishnaswami, S. R. and Gleeson, J. G. (2008). CEP290 interacts with the centriolar satellite component PCM-1 and is required for Rab8 localization to the primary cilium. *Hum. Mol. Genet.* **17**, 3796-3805.

Kim, K., Lee, K. and Rhee, K. (2012). CEP90 is required for the assembly and centrosomal accumulation of centriolar satellites, which is essential for primary cilia formation. *PLoS ONE* **7**, e48196.

Klinger, M., Wang, W., Kuhns, S., Barenz, F., Drager-Meurer, S., Pereira, G. and Gruss, O. J. (2014). The novel centriolar satellite protein SSX2IP targets Cep290 to the ciliary transition zone. *Mol. Biol. Cell* **25**, 495-507.

Knodler, A., Feng, S., Zhang, J., Zhang, X., Das, A., Peranen, J. and Guo, W. (2010). Coordination of Rab8 and Rab11 in primary ciliogenesis. *Proc. Natl. Acad. Sci. USA* **107**, 6346-6351.

Kubo, A., Sasaki, H., Yuba-Kubo, A., Tsukita, S. and Shiina, N. (1999). Centriolar satellites: molecular characterization, ATP-dependent movement toward centrioles and possible involvement in ciliogenesis. *J. Cell Biol.* **147**, 969-980.

Kuhns, S., Schmidt, K. N., Reymann, J., Gilbert, D. F., Neuner, A., Hub, B., Carvalho, R., Wiedemann, P., Zentgraf, H., Erfle, H. et al. (2013). The microtubule affinity regulating kinase MARK4 promotes axoneme extension during early ciliogenesis. *J. Cell Biol.* **200**, 505-522.

Lin, Y.-C., Chang, C.-W., Hsu, W.-B., Tang, C.-J., Lin, Y.-N., Chou, E.-J., Wu, C.-T. and Tang, T. K. (2013). Human microcephaly protein CEP135 binds to hSAS-6 and CPAP, and is required for centriole assembly. *EMBO J.* **32**, 1141-1154.

Lopes, C. A. M., Prosser, S. L., Romio, L., Hirst, R. A., O'Callaghan, C., Woolf, A. S. and Fry, A. M. (2011). Centriolar satellites are assembly points for proteins implicated in human ciliopathies, including oral-facial-digital syndrome 1. *J. Cell Sci.* **124**, 600-612.

Lu, Q., Insinna, C., Ott, C., Stauffer, J., Pintado, P. A., Rahajeng, J., Baxa, U., Walia, V., Cuenca, A., Hwang, Y.-S. et al. (2015). Early steps in primary cilium assembly require EHD1/EHD3-dependent ciliary vesicle formation. *Nat. Cell Biol.* **17**, 228-240.

Mottier-Pavie, V. and Megraw, T. L. (2009). Drosophila bld10 is a centriolar protein that regulates centriole, basal body, and motile cilium assembly. *Mol. Biol. Cell* **20**, 2605-2614.

Ohta, T., Essner, R., Ryu, J. H., Palazzo, R. E., Uetake, Y. and Kuriyama, R. (2002). Characterization of Cep135, a novel coiled-coil centrosomal protein involved in microtubule organization in mammalian cells. *J. Cell Biol.* **156**, 87-100.

Pazour, G. J., Baker, S. A., Deane, J. A., Cole, D. G., Dickert, B. L., Rosenbaum, J. L., Witman, G. B. and Besharse, J. C. (2002). The intraflagellar transport protein, IFT88, is essential for vertebrate photoreceptor assembly and maintenance. *J. Cell Biol.* **157**, 103-114.

Qin, H. (2012). Regulation of intraflagellar transport and ciliogenesis by small G proteins. *Int. Rev. Cell. Mol. Biol.* **293**, 149-168.

Rothbauer, U., Zolghadr, K., Muyldermans, S., Schepers, A., Cardoso, M. C. and Leonhardt, H. (2008). A versatile nanotrap for biochemical and functional studies with fluorescent fusion proteins. *Mol. Cell. Proteomics* **7**, 282-289.

Schmidt, K. N., Kuhns, S., Neuner, A., Hub, B., Zentgraf, H. and Pereira, G. (2012). Cep164 mediates vesicular docking to the mother centriole during early steps of ciliogenesis. *J. Cell Biol.* **199**, 1083-1101.

Shen, K.-F. and Osmani, S. A. (2013). Regulation of mitosis by the NIMA kinase involves TINA and its newly discovered partner, An-WDR8, at spindle pole bodies. *Mol. Biol. Cell* **24**, 3842-3856.

Sillibourne, J. E., Hurbain, I., Grand-Perret, T., Goud, B., Tran, P. and Bornens, M. (2013). Primary ciliogenesis requires the distal appendage component Cep123. *Biol. Open* **2**, 535-545.

Singla, V. and Reiter, J. F. (2006). The primary cilium as the cell's antenna: signaling at a sensory organelle. *Science* **313**, 629-633.

Sonnen, K. F., Schermelleh, L., Leonhardt, H. and Nigg, E. A. (2012). 3D-structured illumination microscopy provides novel insight into architecture of human centrosomes. *Biol. Open* **1**, 965-976.

Spektor, A., Tsang, W. Y., Khoo, D. and Dynlacht, B. D. (2007). Cep97 and CP110 suppress a cilia assembly program. *Cell* **130**, 678-690.

Tanos, B. E., Yang, H.-J., Soni, R., Wang, W.-J., Macaluso, F. P., Asara, J. M. and Tsou, M.-F. B. (2013). Centriole distal appendages promote membrane docking, leading to cilia initiation. *Genes Dev.* **27**, 163-168.

Tollenaere, M. A. X., Mailand, N. and Bekker-Jensen, S. (2015). Centriolar satellites: key mediators of centrosome functions. *Cell. Mol. Life Sci.* **72**, 11-23.

Toya, M., Sato, M., Haselmann, U., Asakawa, K., Brunner, D., Antony, C. and Toda, T. (2007). Gamma-tubulin complex-mediated anchoring of spindle microtubules to spindle-pole bodies requires Msd1 in fission yeast. *Nat. Cell Biol.* **9**, 646-653.

Tsang, W. Y., Bossard, C., Khanna, H., Peranen, J., Swaroop, A., Malhotra, V. and Dynlacht, B. D. (2008). CP110 suppresses primary cilia formation through its interaction with CEP290, a protein deficient in human ciliary disease. *Dev. Cell* **15**, 187-197.

Westlake, C. J., Baye, L. M., Nachury, M. V., Wright, K. J., Ervin, K. E., Phu, L., Chalouni, C., Beck, J. S., Kirkpatrick, D. S., Slusarski, D. C. et al. (2011). Primary cilia membrane assembly is initiated by Rab11 and transport protein particle II (TRAPPII) complex-dependent trafficking of Rabin8 to the centrosome. *Proc. Natl. Acad. Sci. USA* **108**, 2759-2764.

Wolff, A., de Nechaud, B., Chillet, D., Mazarguil, H., Desbruyeres, E., Audebert, S., Edde, B., Gros, F. and Denoulet, P. (1992). Distribution of glutamylated alpha

and beta-tubulin in mouse tissues using a specific monoclonal antibody, GT335. *Eur. J. Cell Biol.* **59**, 425-432.

Ye, X., Zeng, H., Ning, G., Reiter, J. F. and Liu, A. (2014). C2cd3 is critical for centriolar distal appendage assembly and ciliary vesicle docking in mammals. *Proc. Natl. Acad. Sci. USA* **111**, 2164-2169.

Yukawa, M., Ikebe, C. and Toda, T. (2015). The Msd1-Wdr8-Pkl1 complex anchors microtubule minus ends to fission yeast spindle pole bodies. *J. Cell Biol.* **209**, 549-562.

Zhang, C. and Zhang, F. (2015). The multifunctions of WD40 proteins in genome integrity and cell cycle progression. *J. Genomics* **3**, 40-50.